Copyright Warning & Restrictions

The copyright law of the United States (Title 17, United States Code) governs the making of photocopies or other reproductions of copyrighted material.

Under certain conditions specified in the law, libraries and archives are authorized to furnish a photocopy or other reproduction. One of these specified conditions is that the photocopy or reproduction is not to be "used for any purpose other than private study, scholarship, or research." If a, user makes a request for, or later uses, a photocopy or reproduction for purposes in excess of "fair use" that user may be liable for copyright infringement,

This institution reserves the right to refuse to accept a copying order if, in its judgment, fulfillment of the order would involve violation of copyright law.

Please Note: The author retains the copyright while the New Jersey Institute of Technology reserves the right to distribute this thesis or dissertation

Printing note: If you do not wish to print this page, then select "Pages from: first page # to: last page #" on the print dialog screen

INFORMATION TO USERS

This manuscript has been reproduced from the microfilm master. UMI films the text directly from the original or copy submitted. Thus, some thesis and dissertation copies are in typewriter face, while others may be from any type of computer printer.

The quality of this reproduction is dependent upon the quality of the copy submitted. Broken or indistinct print, colored or poor quality illustrations and photographs, print bleedthrough, substandard margins, and improper alignment can adversely affect reproduction.

In the unlikely event that the author did not send UMI a complete manuscript and there are missing pages, these will be noted. Also, if unauthorized copyright material had to be removed, a note will indicate the deletion.

Oversize materials (e.g., maps, drawings, charts) are reproduced by sectioning the original, beginning at the upper left-hand corner and continuing from left to right in equal sections with small overlaps.

Photographs included in the original manuscript have been reproduced xerographically in this copy. Higher quality 6" x 9" black and white photographic prints are available for any photographs or illustrations appearing in this copy for an additional charge. Contact UMI directly to order.

Bell & Howell Information and Learning
300 North Zeeb Road, Ann Arbor, MI 48106-1346 USA

UMI®
800-521-0600

IN-LINE MEASUREMENT OF SOLUBILITY OF PHYSICAL BLOWING AGENTS IN THERMOPLASTIC MELTS AS RELATED TO EXTRUSION FOAMING

by
Qiang Zhang

A Dissertation
Submitted to the Faculty of
New Jersey Institute of Technology
In Partial Fulfillment of the Requirements for the Degree of
Doctor of Philosophy in Chemical Engineering

Department of Chemical Engineering,
Chemistry, and Environmental Science

January 2000

APPROVAL PAGE

IN-LINE MEASUREMENT OF SOLUBILITY OF PHYSICAL BLOWING AGENTS IN THERMOPLASTIC MELTS AS RELATED TO EXTRUSION FOAMING

Qiang Zhang

Dr. Marino Xanthos, Dissertation Advisor — Date
Professor of Chemical Engineering, NJIT

Dr. Dana E. Knox, Committee Member — Date
Associate Professor of Chemical Engineering, NJIT

Dr. Costas G. Gogos, Committee Member — Date
Research Professor of Chemical Engineering, NJIT

Dr. Gordon Lewandowski, Committee Member — Date
Distinguished Professor of Chemical Engineering, NJIT

Dr. Donald H. Sebastian, Committee Member — Date
Professor of Industrial and Manufacturing Engineering, NJIT

Dr. David B. Todd, Committee Member — 9 Dec 1999
Principal Consultant, Polymer Processing Institute — Date

ABSTRACT

IN-LINE MEASUREMENT OF SOLUBILITY OF PHYSICAL BLOWING AGENTS IN THERMOPLASTIC MELTS AS RELATED TO EXTRUSION FOAMING

by
Qiang Zhang

A novel in-line method for measuring physical blowing agent solubility in thermoplastic melts in extrusion foaming equipment has been developed in this study. This method uses video microscopy in connection with a foaming extruder (single or twin-screw) to generate solubility data by observing the onset of gas bubble formation/dissolution. This method offers a number of advantages over the existing conventional methods. It can be easily used to obtain solubility data for many foamable thermoplastic-physical blowing agent systems at high pressure and temperature near actual foaming conditions. Data generated using this method could be directly used to characterize and control a foaming process and also provide guidelines for blowing agent selection, foam process design and optimization.

Solubility data of three different inert gases, CO_2, Ar and N_2, in polystyrene under different temperatures have been obtained. Overall, the results compare favorably with literature equilibrium data obtained with off-line methods. Solubility data of the same gases in polyethylene terephthalate have also been generated. To the author's knowledge, solubility data for this system at melt temperatures are not currently available in the literature. Data obtained from the twin-screw extrusion experiments show much better consistency compared with those obtained from single screw experiments; this indicates

the importance of enhanced mixing in affecting the solubility values obtained from the in-line method.

A simple surface renewal model is used to study the gas dissolution behavior over the gas injection section during the foaming process. The model was found insufficient to explain the very complex phenomena occurring inside the extruder, suggesting the existence of other mechanisms that contribute to gas dissolution over the entire extruder length.

The effects of processing conditions on solubility and gas dissolution characteristics are studied using the in-line window system with a co-rotating twin-screw extruder. The results show that the measured CO_2 take-up values in polystyrene are affected by polymer throughput, suggesting that an "apparent solubility" is measured.

Gas solubility and dissolution results are applied to analyze the extrusion foaming process in which a commercially available polyethylene terephthalate is foamed in a single screw extruder by injection of atmospheric gases (CO_2, Ar and N_2) that were shown to exhibit different degrees of solubility. The results and their general implication on the extrusion foaming process of thermoplastics are discussed.

BIOGRAPHICAL SKETCH

Author: Qiang Zhang

Degree: Doctor of Philosophy

Date: January 2000

Undergraduate and Graduate Education:

- Doctor of Philosophy in Chemical Engineering
  New Jersey Institute of Technology, New Jersey, 2000
- Master of Science in Chemical Engineering
  University of Wyoming, Laramie, Wyoming, 1994
- Master of Science in Chemical Engineering
  Beijing Institute of Chemical Technology, Beijing, China, 1989
- Bachelor of Science in Chemical Engineering
  Hebei Institute of Chemical Technology, Hebei, China, 1983

Major: Chemical Engineering

Presentations and Publications:

Xanthos, M., S. K. Dey, Q. Zhang and J. Quintans, " Parameters Affecting Extrusion Foaming of PET by Gas Injection", *Proceedings of the 57th SPE ANTEC*, New York, NY, pp2109-2113, May 3-6, 1999.

Zhang, Q., M. Xanthos and S. K. Dey, "In-Line Measurement of Gas Solubility in Polystyrene and Polyethylene Terephthalate Melts during Foam Extrusion", *Porous, Cellular and Microcellular Materials*, MD-Vol. 82. 1998 ASME International Mechanical Engineering Congress and Exposition, Anaheim, CA, pp75-83, Nov. 15-20, 1998.

Xanthos, M., Q. Zhang, S. K. Dey, Y. Li, U. Yilmazer and M. O'Shea, "Effects of Resin Rheology on the Extrusion Foaming Characteristics of PET", *Journal of Cellular Plastics*, Vol. 34, 498-510, 1998.

Xanthos, M., S. K. Dey and Q. Zhang, "Sheet Extrusion of Polyethylene Terephthalate", *Proceedings of the 1998 Polymers, Laminations and Coatings Conference (TAPPI)*, San Francisco, CA, pp645-650, August 30-September 3, 1998.

Xanthos, M., S. K. Dey and Q. Zhang, "Production of PET Foam with Viscosity Modifier", *Proceedings of the FoamPlas'98 Conference*, Teaneck, NJ, pp9-13, May 1998.

Dey, S. K., Q. Zhang, N. Faridi and M. Xanthos, "Measurements of Gas Solubility in Thermoplastic Melts During Foam Extrusion", *Proceedings of the 55th SPE ANTEC*, Toronto, Canada, pp1988-1990, May 1997.

Faridi, N., S. K. Dey, M. Xanthos and Q. Zhang, "On-line and Off-line Solubility Measurements in Foamable Thermoplastics", *Proceedings of the 13th Polymer Processing Society International Conference*, p11-B, Secaucus, New Jersey, June 1997.

This dissertation is dedicated to
my wife Hua and my sons William and Albert

ACKNOWLEDGMENT

I would like to express my deepest appreciation to Dr. Marino Xanthos, my research advisor, for his constructive guidance, valuable suggestions and constant support and encouragement throughout this project without which this work would not have been possible. Special thanks are due to each of my committee members, Dr. Dana E. Knox, Dr. Costas G. Gogos, Dr. Gorden Lewandowski, Dr. Donald H. Sebastian and Dr. David B. Todd for all the suggestions made.

Partial financial support provided by the Multi-lifecycle Engineering Research Center (MERC) at the New Jersey Institute of Technology is highly appreciated. Thanks are also due to Dow Chemical Company for providing the polystyrene material. The assistance of Dr. Forest Busby and Dr. Jim Chou of Dow Chemical Company is greatly appreciated.

I am very grateful to Dr. Subir K. Dey of the Polymer Processing Institute (PPI) not only for his help in making me understand and starting off this work, but also for providing insights and making constructive suggestions throughout this work.

I am also grateful to my current and former fellow students, Mr. Chaiya Chandavasu and Mr. Yufu Li for their unconditional help and encouragement.

I specially thank Dr. Victor Tan, Dr. Niloufar Faridi, and Mr. Dale Conti of PPI for their technical assistance. I am grateful to Mr. Yogi Gandhi of the Chemistry laboratory for his generous help in providing innumerable laboratory items.

I take this opportunity to thank my wife for her support, endurance and understanding. I am very grateful to my children for bringing so much joy to my life which truly made this long journey enjoyable.

TABLES OF CONTENTS

TABLES OF CONTENTS
(Continued)

TABLES OF CONTENTS
(Continued)

LIST OF TABLES

LIST OF FIGURES

LIST OF FIGURES
(Continued)

LIST OF FIGURES
(Continued)

Figure **Page**

NOMENCLATURE

a	Mass transfer area (cm^2)
a_{bf}	Surface area of the melt rolling pool (cm^2)
a_{pf}	Surface area of the barrel film (cm^2)
a_i	Incremental surface area (cm^2)
A	System-dependent parameter for nucleation rate calculation
b	System-dependent parameter for nucleation rate calculation
c	Gas concentration in polymer melt (g/cm^3)
c_e	Equilibrium gas concentration (g/cm^3)
c_i	Initial concentration (g/cm^3)
C_a	Capillary number (dimensionless)
C_a^c	Critical capillary number (dimensionless)
D	Screw diameter (cm)
D_{AB}	Diffusivity of component A in component B (cm^2/s)
E_{BA}	Blowing agent efficiency (dimensionless)
E_S	Heat of solution (J/mol)
f	Degree of fill of the screw channel (dimensionless)
H	Extruder screw channel height (cm)
Hw	Henry's law constant (cm^3 [STP]/g•kPa)
H_{W0}	Henry's law constant at reference temperature, T_0 (cm^3 [STP]/g•kPa)
k	Boltzmann constant (dyne cm/K)
L	Screw length (cm)

NOMENCLATURE
(Continued)

m_g	Gas dissolution rate (g/s)
m_p	Polymer throughput (g/s)
n	Rate of gas dissolution (g/cm^3s)
$\bar{n}$	Average mass flux (g/cm^3s)
n_a	Gas dissolution rate per unit area (g/cm^2s)
N	Screw speed (rpm)
N_r	Bubble nucleation rate
P	Melt pressure (kPa)
P_{inside}	Pressure inside the bubble (kPa)
P_{melt}	Pressure in the melt pool (kPa)
ΔP	difference between the ambient and the gas vapor pressure (kPa)
r	Bubble radius (μm)
R	Cavity mouth radius (cm)
R^c	Critical radius (cm)
$\dot{r}$	Bubble growth rate (cm/s)
S	Gas solubility (cm^3 [STP]/g)
t	Time (s)
t_d	Characteristic diffusion time (s)
t_e	Exposure time (s)
Δt_e	Incremental time (s)
t_{be}	Renewal time for the barrel film in the screw channel (s)

NOMENCLATURE
(Continued)

t_{pe}	Renewal time for the rolling pool in the screw channel (s)
T	Absolute temperature (K)
T_c	Critical temperature of the solute (K)
V_{BZ}	Down channel velocity (cm/s)
$\overline{V}_{BZ}$	Average Down channel velocity (cm/s)
V_{BX}	Cross channel velocity (cm/s)
V_S	Melt circular flow velocity (cm/s)
w	Gas weight fraction (dimensionless)
w_i	Initial gas weight fraction (dimensionless)
w_e	Equilibrium gas weight fraction (dimensionless)
W	Extruder screw channel width (cm)
Δz	Incremental down channel step (cm)
$\dot{\gamma}$	Shear rate (s^{-1})
$\overline{\dot{\gamma}}$	Average shear rate (s^{-1})
η	Liquid viscosity (Pa•s)
η_0	Zero-shear viscosity (Pa•s)
δ	Flight clearance (cm)
ρ	Density of the gas-laden melt (g/cm^3)
σ	Surface tension (dyne/cm)
τ_{rr}	Shear stress at the interface between the expanding gas and the melt ($dyne/cm^2$)
ϕ	Screw helix angle (rad)

CHAPTER 1

INTRODUCTION

1.1 Polymer Foams and Their Environmental Problems

Polymeric foams are materials of great commercial importance. At lower densities, these materials possess thermal insulation properties that compare favorably with well-known insulating materials such as glass fibers. At higher densities, they offer substantial material and weight savings in structural applications where rigidity is required.

Polymeric foams comprise a wide variety of materials. Their main applications include furniture, transportation, bedding, carpet underlay, packaging, textiles, toys and novelties, gaskets, sports applications, shoes, shock-and sound-absorbing applications (automobiles, shoe inserts, etc.), insulation, appliances, flotation, decorative moldings, food and drink containers, and business machine housings, among others. Lowest density foams are used in packaging applications and refrigeration insulation, while higher density foams are used for load-bearing structural applications (Klempner and Frisch, 1991).

Since their introduction in the early 1950's, foamed polymeric products have been playing a crucial role in advancing technologies from automotive, construction, to almost every aspect of everyday life. According to the "Modern Plastics" 1998 Resins Report, the 1997 U.S. consumption of polyurethane foams reached 3449 million pounds. On the thermoplastic side, in 1997, the consumption of foamed polystyrene alone reached 916 million pounds, up 4% from 1996. As the traditional foamed products find new applications, some relatively new materials have been foamed and continue to grow at a fast pace. A number of thermoplastic foams have been available through various foaming technologies in the market for a long time. Their densities range from 0.8 g/cm^3 to less

than 0.01 g/cm^3, depending upon the foaming method and the combination of foaming agents and the thermoplastic resin.

Thermoplastic foams can be produced by many different processes, the most popular ones being injection molding and extrusion. In the extrusion process, the extruder offers relevant unit operations for foam production, such as melting, mixing and metering in a continuous mode.

Two kinds of blowing agents have been used for continuous foam extrusion of polymeric materials, namely, chemical blowing agents (CBAs) and physical blowing agents (PBAs). Chemical blowing agents decompose at processing temperature and generate gas or gases necessary for foaming; physical blowing agents are dissolved into the polymer melt in the extruder before exiting the die. Physical blowing agents usually have the advantage of making lower density foams than the thermally activated chemical blowing agents.

The foremost problem facing the foaming industry in the last ten to fifteen years has been the phasing out of some of its physical blowing agents. The polymer foaming industry has been one of the major industries that uses and releases ozone-depleting substances (ODS). According to U.S. EPA's estimation (Anonymous, 1994), in the United States, foam plastics accounted for approximately 18% of all U.S. consumption of ozone-depleting chemicals in 1990. Continuous extrusion foaming processes primarily used chlorofluorocarbons (CFC) as blowing agents, prior to their recent ban. The release of chlorofluorocarbons (CFCs) and other ozone-depleting substances (ODS) are causing rapid erosion of the stratospheric ozone layer. The United Nations Environmental Program (UNEP) has earlier estimated that by the year 2000, total global ozone could be

reduced by as much as ten percent (Anonymous, 1997). Ozone depletion allows greater amounts of UV-B radiation to reach the Earth's surface, posing serious consequences to human health. UNEP estimates (Anonymous, 1997) that a sustained ten percent loss of ozone would lead to a twenty-six percent increase in the number of cases of non-melanoma skin cancer per year worldwide. At the same time, 1.6 million additional cataract cases per year would occur. Excessive exposure to UV-B rays is also suspected to suppress human and animal immune systems (Anonymous, 1997). Following the ban on use of CFCs for the foam production in January, 1996, the foam industry ventured to other groups of chemicals. Currently, hydrochlorofluorocarbons (HCFCs), Hydrofluorocarbons (HFCs) and volatile organic compounds (VOCs), mostly hydrocarbons are the major chemicals being used as blowing agents.

HCFCs are also ozone-depleting chemicals, and are used only as transitional alternatives to CFCs facing a year 2030 deadline for complete phase-out. A two-year animal toxicity study at DuPont (Anonymous, 1992) has shown that 2,2-dichloro-1,1,1-trifluroethane (HCFC-123), a major CFC substitute as a foam blowing agent, contributed to the development of nonmalignant tumors in rats. As the result, Dupont lowered their Acceptance Exposure Limit (AEL) for HCFC-123 to 10 parts per million (ppm)-a level far below the limit formally allowed for CFCs. Alternatives such as HFCs and VOCs also have adverse environmental effects and safety problems due to their flammability, toxicity, and global warming potentials and may pose danger to industrial workers and consumers.

Another very important aspect of the problem is that foams manufactured by these agents release those harmful chemicals during the entire lifetime of the products. Research has shown (Kesari et al., 1995) that significant amounts of CFCs are trapped over long

periods in polystyrene and polyurethane foams. Initial concentrations of CFCs in such foams are in the 20-30 wt. % range; in the absence of free exchange with air, these foams effectively retain CFC for long periods of time. Polyurethane samples from 15-year old refrigerators were found to contain CFC at concentrations ranging from 15-20 wt. % (Kesari et al., 1995). The same researchers concluded that these foams represent a large, long-term source of CFCs in the environment. This means that foams made with harmful chemicals (including HCFCs, HFCs and VOCs) today may adversely affect the environment and people's health for the next 15-30 years. So, there is an urgent need to find long term, environmentally friendly alternative foaming agents for the production of polymeric foams.

1.2 Recent Trends in Using Inert Gases as Alternative Physical Blowing Agents

In response to increasing regulation of halocarbons and increasing safety and environmental concerns over the use of flammable, volatile hydrocarbons (VOC), recent research focused towards replacing the traditional foaming agents with various inert gas blowing agents such as CO_2, N_2, Ar, etc. Currently, CO_2 is being commercially used as blowing agent in polyurethane foaming along with CFC alternatives such as HCFC and HFC. Some thermoplastic foaming processes using CO_2 (Gabriele, 1996) and other atmospheric gases as blowing agents have also been developed while most thermoplastic foams are still being manufactured using HCFCs and hydrocarbons as blowing agents.

The use of inert gases in foam extrusion has been shown to demand a very narrow window of processing conditions as opposed to the use of halocarbons (Jacob and Dey, 1995). Inert gases are also much less soluble in the polymer melt and have much higher

vapor pressures than CFCs or hydrocarbons. A very important parameter in the production of these multi-component, multiphase systems is the solubility of physical blowing agents in the pressurized polymer melt, as affected by concentration, pressure and temperature. A knowledge of the solubility characteristics of the gas in polymer melts is highly desirable in order to estimate the pressure requirements to keep it in the melt throughout the extruder all the way to the die, thus avoiding the formation of premature bubbles which would result in uneven cell growth.

1.3 The Importance of Physical Blowing Agent Solubility

Physical Blowing Agents (PBAs) are metered and dissolved in the polymer melt during extrusion processing. As the gas-laden melt emerges from the die it experiences a sudden pressure drop; this thermodynamic instability causes a phase separation. It is believed that bubble nucleation is heterogeneous and begins inside the shaping die (Throne, 1996). The escaping gas leads to expansion within the fluid matrix in such a manner that individual bubbles grow and merge into cells and through subsequent solidification, stable expanded structures are produced. Application of inert gas foaming in a variety of extruded polymers have been described in a number of publications (Boone, 1996; Dey, et al., 1996a; Dey, et al., 1996b; Jacob and Dey, 1995; Xanthos, et al., 1998).

The solubility and diffusivity of the gas in the melt, the interfacial tension, the viscoelastic properties of the molten polymer, and its ability to crystallize, are among material parameters playing an important role during the various stages of extrusion foaming. Both gas solubility and diffusivity influence nucleation and growth of cells. Nucleation rate depends on surface tension of polymer and thus is affected by the presence

of dissolved gas. Bubble growth is also a function of diffusion coefficient, solubility and gas concentration, and melt viscosity and elasticity. Earlier experiments attributed differences in nucleation behavior to differences in solubility of PBA in two different PPs (Cheung, et al., 1996). Dissolution of PBAs in extruders is affected by solubility, diffusivity, pressure, mixing and residence time. PBAs need to be highly soluble and remain in solution throughout the extrusion process. High solubility implies incorporation of sufficient quantities of gas at process temperatures to reach the target densities. Low solubility implies that very high extrusion pressure and fairly high injection pressures are required to achieve very low foam densities, particularly for thicker foam sheets. It is generally recognized that only a soluble amount of gas should be injected into the polymer melt stream with excess gas being detrimental to the cell structure. Undissolved microbubbles may promote premature nucleation and bubble growth before the melt exits the die, and overall unstable foaming that will affect the product microstructure and surface texture (Park, et al., 1997; Xanthos, et al., in press). Compared with CFCs, HCFCs and hydrocarbons, the solubility of atmospheric gases in the pressurized melt of commodity foamable polymers, (polyolefins, polystyrene), is rather limited; this necessitates the use of very high extrusion foaming pressures when inert gases are used as blowing agents. Solubility and diffusivity will also significantly influence the long-term foam characteristics, since diffusion of the blowing agent out of the cells and polymer matrix (which will proceed continuously during the entire life time of the foamed product) will affect the thermal and mechanical properties of the foam (Moulinie et al., 1998).

1.4 Dissolution and Solubility of Gases in Polymer Melts

Data on gas solubility in polymer melts have been reported by many investigators. (Newitt and Weale, 1948; Lundberg, et al., 1963; Durrill and Griskey, 1966; 1969; Dagli et al., 1989). Most of these experiments were carried out in batch where only thermodynamic equilibrium data could be obtained. Due to difficulties encountered in various measurement methods, only limited data are available for certain polymer-gas systems with most of the data being obtained at temperatures below the glass transition temperatures of the polymers involved. A close examination of the data from different sources shows that those data are often inconsistent. For example, opposite temperature dependence has been reported for the same system (Polystyrene-N_2) by different research groups employing different methods. Daigneault and coworkers (1997) have reported two sets of solubility data on Polystyrene-HFC134a system at 120 °C obtained in the same laboratory using two different methods; over 100% difference between the two sets of data was reported. Moreover, solubility data are not available for many polymer-gas systems, especially those involving polymers with high melting points, mainly due to difficulties involved in high temperature measurements. Furthermore, data obtained from off-line measurements may not be suitable to characterize and control the foam extrusion process, since it is possible that equilibrium has not been attained within the residence time in the extruder. Also, the dynamic nature of the extrusion process may play an important role in bubble nucleation/gas dissolution in the polymer melt.

The basic steps in a foaming process involve dissolution of the blowing agent into the polymer melt, which is a diffusion controlled process, followed by expansion through the nucleation and growth of bubbles, which is generally achieved by suddenly releasing

system pressure, and finally stabilization of the resultant cellular structure, which is accomplished by subsequent cooling and solidification of the cell walls.

Considerable research of a theoretical and experimental nature has been conducted on processes that involve the formation and growth of gas bubbles in polymer solutions/melts during foam formation or devolatilization of polymer solutions. Mass transfer processes in extruders during polymer devolatilization have also been studied to some detail. However, studies on gas dissolution processes in extruders during foam extrusion have been largely ignored, likely due to the fact that when traditional blowing agents are used, gas dissolution has never been a major concern thanks to the high solubility of those agents. As discussed earlier, when inert gases are used as blowing agents, the system needs to operate at much higher pressures, and gas solubility and dissolution become major factors in determining the process efficiency/feasibility and product quality. Thus, it is highly desirable to have a better understanding of gas dissolution mechanisms and their relation to processing conditions and machine design parameters.

1.5 Proposed Work

In this study, a novel in-line method is developed by integrating video microscopy with a foaming extruder with optical windows installed at the end of the extruder. The system is first tested for a polystyrene-CO_2 system for ease of operation and availability of literature data. Upon confirming the feasibility of the method, the system is used to measure solubility data for polymer-gas systems involving an amorphous polymer (polystyrene) and a semicrystalline polymer (polyethylene terephthalate) and three different inert gases (CO_2,

N_2 and Ar). The effects of temperature on solubility is studied in small temperature ranges and compared with literature results.

Gas dissolution mechanisms are discussed and analyzed using a penetration mass transfer model combined with a surface renewal melt model developed by researchers in analyzing mass transfer in polymer devolatilization processes. Emphasis will be on a single screw extruder system. An intermeshing co-rotating twin-screw extruder will also be used for solubility measurements. Given the versatile nature of the twin-screw extruder, emphasis here is on the study of possible effects of processing conditions, including enhanced mixing, on the gas solubility and dissolution characteristics. Parameters including screw speed and polymer throughput are varied in large ranges for these studies.

First, this dissertation will cover the background available in the necessary areas of foam extrusion, solubility measurements and interfacial mass transfer into liquid films. The development of the new in-line method will be outlined with detailed descriptions of experimental equipment and procedures. The theoretical basis of this method will also be presented followed by a discussion of the experimental results. At that point the discussion will turn to the gas dissolution analysis. A description of the modeling will be followed by a quantitative analysis. Results on the effects of processing conditions on solubility and gas dissolution characteristics will then be presented and discussed followed by a conclusive summary.

CHAPTER 2

BACKGROUND

2.1 Extrusion Foaming by Gas Injection

Extrusion is one of the most popular processes used in foaming polymeric materials. This process can use a single extruder or more commonly, two extruders operating in tandem. The schematics of single barrel and tandem foam extruders are given in Figure 2.1. In the single extruder case, a high length to diameter ratio equipment is normally required to provide enough elements for polymer melting, gas dissolution, sufficient cooling and pressurization, and foaming through the die. In such a process typically a two-stage screw is used. The polymer composition fed in the extruder feed section is melted and mixed in the transition section of the screw and then the blowing agent is injected. The blowing agent is dispersed and dissolved in the melt; this process depends on several factors including the type of the resin and blowing agent, temperature, pressure and other operating conditions. The gas-laden melt is then pressurized and extruded through the die. The temperature profile on the extruder is set in such a way that for the zones prior to the gas injection, the temperature is high enough to ensure proper melting; for the zones past the injection section, temperature is gradually lowered substantially so as to allow for adequate cooling of the gas-laden melt prior to exiting the die, a necessary condition for cell expansion without coalescence.

In the tandem process, the polymer and additives are melted and mixed in a primary extruder, which is typically equipped with a high shear mixing screw. The blowing agent is injected near the end of this primary extruder, the blowing agent-containing melt is then transferred to the feed section of the secondary extruder through

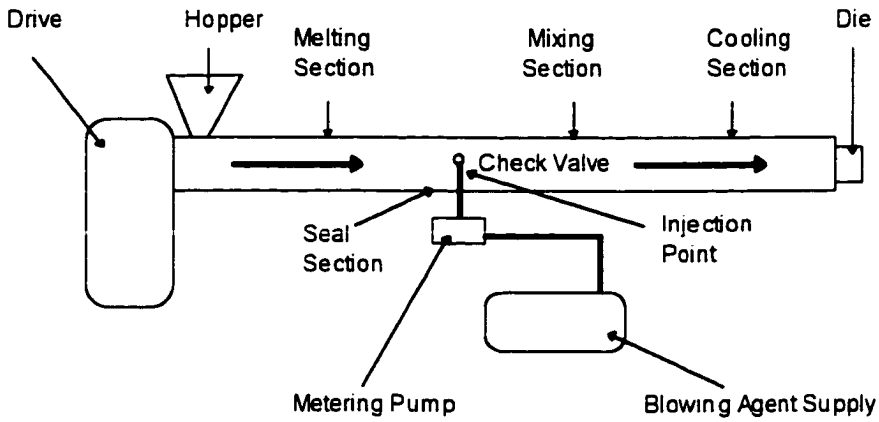

Single (Large L/D)

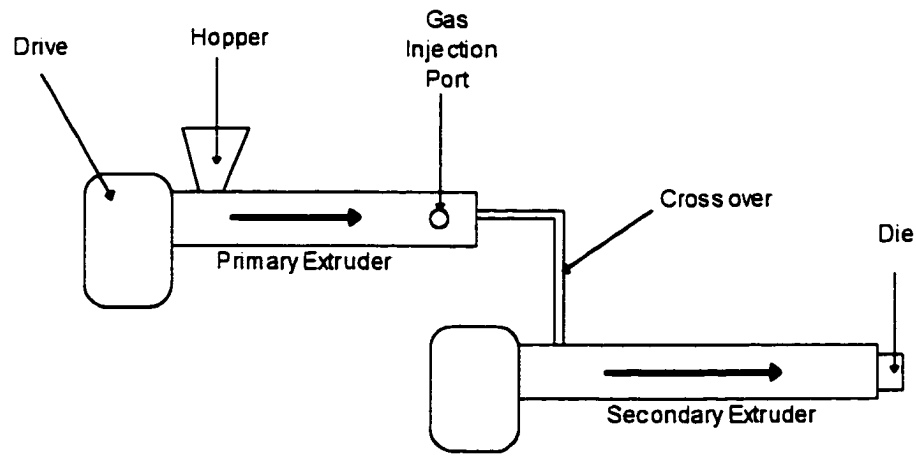

Tandem

Figure 2.1 Schematics of Single Barrel and Tandem Foam Extruders

the so-called crossover section. The main purpose of the secondary extruder is to cool the gas-laden melt to an optimum melt temperature and pressure for foam formation without cell coalescence. The tandem extruder set-up normally allows for excellent control of process variables, and is used in industry to produce very low-density foams.

The basic requirements on polymer, the blowing agent(s), nucleator(s), equipment and processing parameters for making extruded polymeric foam are shown schematically in Figure 2.2 (Based on reference by Khemani, 1997).

The first requirement for successful foaming is to form a uniform gas-laden melt. This means that all gas molecules are dispersed on a molecular level throughout the melt. The key here is the solubility of the gas in the polymer at the melt temperature. Most polymer-gas systems show a linear relationship between solubility, S [cm^3(STP)/g], and gas pressure, P (kPa), at a given temperature:

$$S = Hw \times P \tag{2.1}$$

Where Hw is the Henry's law constant [cm^3(STP)/g kPa] which normally shows an Arrhenius type of temperature dependence. Certainly, the first criterion for successful foaming is to ensure that the gas molecules are dispersed and dissolved in the polymer melt and not residing in microbubbles (Throne, 1996). If low solubility inert gases such as N_2 and Ar are used as blowing agents to produce low-density foams of many commercial polymers, very high extrusion and die pressures are normally required.

The rheological properties of the gas-laden melt become very important; for example, the viscosity of the mixture has to be high enough to achieve the pressure

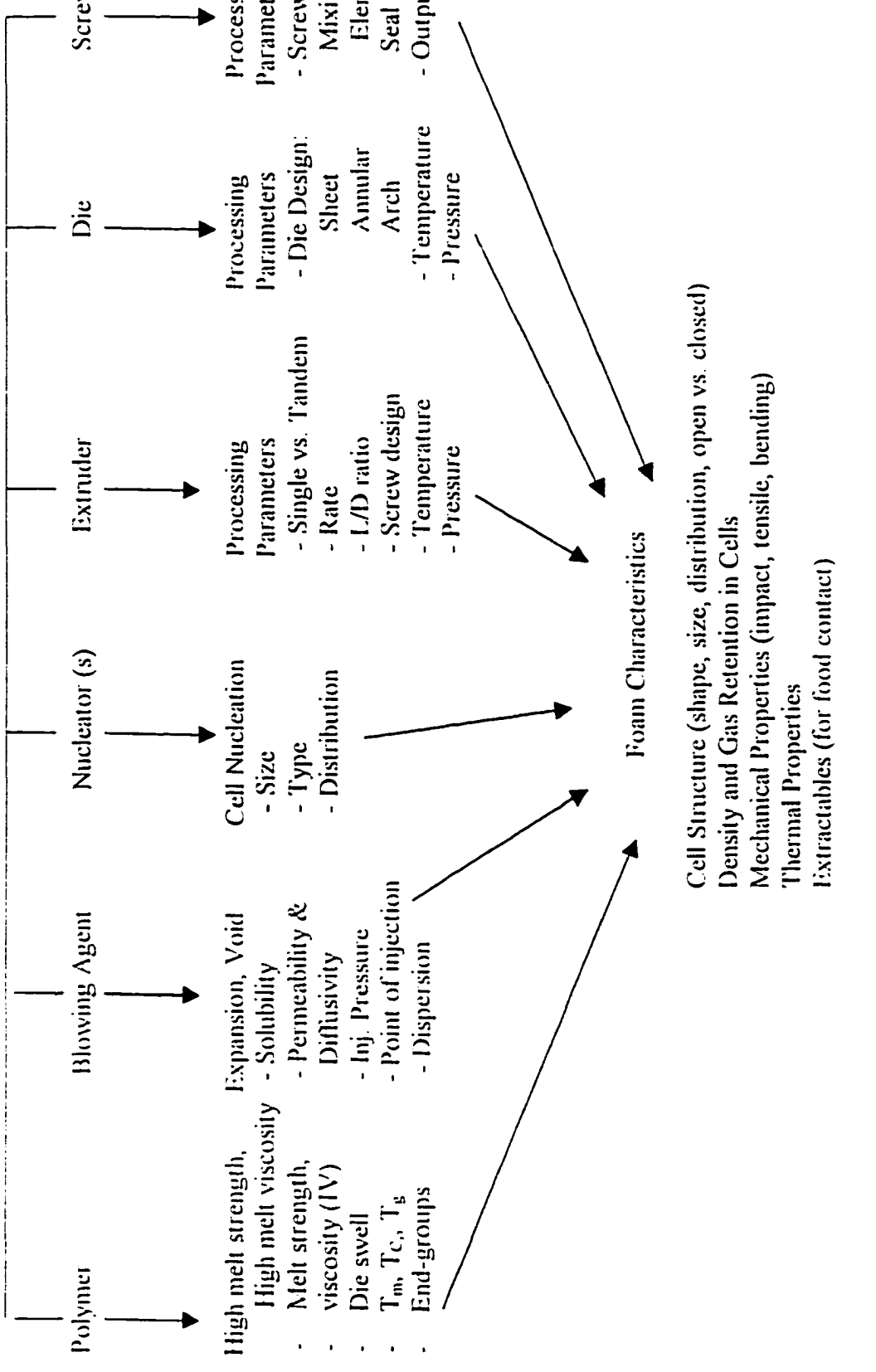

Figure 2.2 Parameters Affecting the Thermoplastics Foam Extrusion Process

required. The viscosity of the gas-laden melt is a strong function of the gas concentration. It has been shown (Throne, 1996) that at a given temperature, the gas-laden polymer melt viscosity decreases essentially linearly with gas content throughout the practical range of gas concentration for many polymer-gas systems. The required high pressure is normally achieved by cooling the polymer-gas mixture substantially before reaching the extrusion die. Temperatures can be set to below the normal polymer melting point and near the crystallization temperatures in cases of semi-crystalline polymers and near T_g for amorphous polymers. This is possible because the inclusion of the gas causes depression of the glass transition temperature (T_g) of an amorphous polymer and the crystallization temperature (T_c) of a semicrystalline polymer. Depression of T_g or T_c is a well-known phenomenon and experimental results are available for a number of polymer-gas systems (Wang et. al., 1982; Wissinger and Paulaitis, 1991; Dey et. al., 1994; Handa at al., 1996; Zhang and Handa, 1997).

Extrusion foaming by gas injection mainly involves gas dissolution through dispersion/mixing and pressurization, bubble nucleation and growth due to super-saturation and diffusion of gas into the nucleated bubbles, and finally stabilization of cell structure by cooling due to vaporization of physical blowing agents. Other material properties that influence these processes include melt shear and elongational viscosity, melt strength, and, if crystallizable, the rate of crystallization. Gas/polymer interfacial properties also play a significant role in affecting all of these stages of operation.

2.1.1 Gas Dissolution inside the Extruder

A large amount of theoretical and experimental research has been conducted on the extrusion processes involving gas-liquid mass transfer. The emphasis has been put on the extruder die end and beyond where gas bubble nucleation and growth occur. Little or no attention has been paid to study the gas dissolution process that takes place in the extruder after gas is injected in the melt. A better understanding of the main mechanisms for gas dissolution will provide guidance to proper process control, design and optimization. This is especially important when inert gases, which normally have very low solubility in polymers, are used as blowing agents, since the use of these gases requires much higher extrusion and die pressure, which, in turn, do not favor foaming efficiency.

Dissolution of physical blowing agents is affected by solubility, diffusivity, pressure, mixing and residence time. Shear forces and interfacial tension may also play a significant role in affecting the gas dissolution process. Some detailed studies on mass transfer mechanisms in extruders have been reported by many researchers for polymer solution devolatilization processes. The devolatilization process resembles the extrusion foaming process in the way that gas-liquid mass transfer happens in a partially filled section of the extruder. The concepts such as polymer flow models and gas-liquid mass transfer models developed and used in devolatilization research can be borrowed to study gas dissolution during the process of extrusion foaming.

The two key process elements operative in all rotating machines used for melt devolatilization have been identified as the rotating melt pool and the stationary melt film (Biesenberger and Sebastian, 1983; Biesenberger, 1983). As shown schematically in Figure 2.3, in extruders the pool rotates in the partially filled channel under the influence

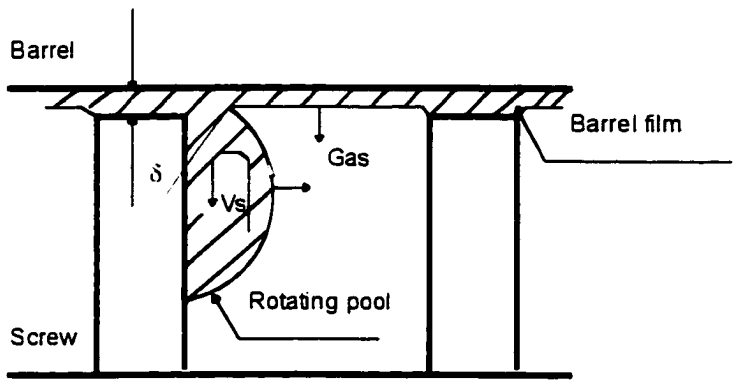

Figure 2.3 Schematic of the Mass Transfer Areas in a Polymer Devolatilization Process

of the cross channel component of the screw velocity, while being conveyed through the extruder in drag flow by the down channel component. A stationary melt film is deposited on the barrel wall due to the clearance between screw and barrel. Most work in equipment design of the extruder has focused on surface renewal of polymer melts in single-screw extruders (Latinen, 1962; Coughlin and Caneveri, 1969; Roberts, 1970; Biesenberger and Kessidis, 1982) and in twin-screw extruders (Collins et. al., 1985; Biesenberger et. al., 1990). These studies used the penetration model for mass diffusion to describe the mass transfer mechanism for polymer devolatilization. Their models relied on the ability of the extruders to continuously generate free surface area available for diffusion of the volatile component from the polymer liquid to the polymer-gas interface and into the contiguous gas phase.

The penetration model basically assumes the mass transfer films to be semi-infinite slabs in which the uni-directional diffusion can be described by:

$$\frac{\partial c}{\partial t} = D_{iB} \frac{\partial^2 c}{\partial x^2} \tag{2.2}$$

The boundary conditions are that the interface is at the equilibrium concentration c_e, the film is initially homogeneous at c_i, and the concentration at large film depth remains at c_i.

The penetration model applies only when surface renewal is rapid enough that only unsteady state mass transfer exists in any fluid element at the surface. Mathematically

speaking, the exposure time of any element should be less than the characteristic time, t_d, for diffusion expressed by:

$$t_d = \frac{x^2}{D_{AB}} \tag{2.3}$$

Where x is the film thickness and D_{AB} is the diffusivity in the mixture of components A and B. Care must be taken when applying the penetration theory since the barrel clearance δ, which dictates the thickness of the barrel film, can vary in the range of 3-10 mil (0.075-0.25 mm) depending on the design and the degree of wear of the extruder. Toor and Marchello (1958) proposed a combined film-penetration model that is applicable to the cases where the exposure times are greater than t_d but less than infinity.

One of the main objectives of this study is to apply these principles to study the gas dissolution during extrusion foaming, and compare the simulation results with experimental data in an attempt to elucidate possible mechanisms involved in gas dissolution inside an extruder after the gas is injected.

2.1.2 Bubble Nucleation, Growth and the Cell Structure Stabilization

The formation of foams starts with bubble nucleation followed by growth of these bubbles by diffusion of gas into existing cells. While the nucleation is normally an instantaneous and relatively isothermal process, the bubble growth happens over time in a highly non-isothermal fashion. A great deal of theoretical and experimental studies on these

phenomena has been conducted over the years. The classical nucleation theory is based on the typical Arrhenius type equation of the form:

$$N_r = A\exp(b/kT) \tag{2.4}$$

This equation has been used to predict nucleation rates, N_r, where A and b are system-dependent parameters and k is Bolzmann's constant. Colton and Suh (1987) used this type of approach to develop individual equations for homogeneous and heterogeneous nucleation for bubble formation in a polymer solution. An expression for the Gibbs energy is used in the exponential term that is related to the surface energy of the polymer-bubble interface and the gas pressure in the bubble. For the heterogeneous case, a term is added to the expression for Gibbs energy that accounts for the effect of the nucleating agent which is based on the wetting angle of the gas-nucleating agent-polymer interface. The total rate of nucleation is the sum of the homogeneous and heterogeneous rates. Colton and Suh (1987) performed a number of experiments in an attempt to validate this model and showed that the model is qualitatively correct. Kumar and Weller (1992) compared their experimental results to the predictions using the Colton and Suh model and concluded that additional work is required to account for the unique nature of polymers. Lee (1993, 1994) studied the shear effects on thermoplastic foam nucleation during extrusion foaming of LDPE with an HCFC blowing agent and talc as nucleating agent. A capillary number that is the ratio of shear force to surface tension force is incorporated into the exponent of the Arrhenius type rate equation. For the system studied, this

approach provided reasonable agreement between the experimental results and the model prediction.

Considerable research has been conducted on the bubble growth mechanisms, which has led to an increased understanding of the processing of polymeric foams. The models available in the literature cover a wide spectrum of physical situations including Newtonian and non-Newtonian fluid behavior, isothermal and non-isothermal conditions, and the bubble growth occurring in either an infinite pool (single bubble model) or in a thinly bounded layer (multiple bubble model). The effect of polymer elasticity was also incorporated in models to study the bubble growth dynamics (Street, 1968; Street et al., 1971). Amon and Denson (1984) developed a cell model that is capable of describing numerous bubbles growing in close proximity to one another under isothermal conditions. The derived equations were solved numerically. Ramesh et al. (1991) extended the theory of bubble growth based on mass and heat transfer to an Ostwald-de Waele power law fluid. Street et al. (1971) also introduced a non-isothermal system where the interfacial temperature was different from the bubble temperature. Ramesh and Malwitz (1997) modified the model by Ramesh et al. (1991) to include the concentration effects. The non-Newtonian nature of the polymer/blowing agent mixture was modeled using the convected Maxwell model. The authors compared their experimental results for a LDPE/n-butane system with their model predictions, and concluded that inclusion of concentration effects into the model is essential to understand foam growth characteristics in industrial foaming processes.

When molten thermoplastics are foamed they are cooled immediately thereafter to provide the necessary increase in viscosity and also modulus. By contrast to atmospheric

gases, higher molecular weight PBAs such as Freons and hydrocarbons provide further ability to stabilize the foams through quenching by vaporization. Further material requirements for structure stabilization include: moderately high elongational viscosity to allow biaxial stretching of the cells, high melt strength to resist membrane tearing (blow-out) and promote the formation of closed-cell structures, and, if crystallizable, relatively rapid rate of crystallization.

2.2 Solubility of Gases in Molten or Thermally Softened Polymers

2.2.1 Main Factors Affecting Gas Solubility

For molten polymers, the solubility of a blowing agent dictates the conditions under which bubbles will start to nucleate and grow. After the foaming process, the long-term characteristics of the foam are still influenced by the solubility and diffusivity of the blowing agents. Diffusion of the blowing agent out of the cells and polymer matrix will change the thermal and mechanical properties of the foam. This is especially the case when the blowing agent plasticizes the polymer, and the material stiffens as the blowing agent diffuses out (Moulinie et. al., 1998).

It is generally accepted that solubility is dependent on the free volume available to the gas molecules in the polymer, and therefore dependent on temperature and pressure. Free volume increases with temperature, therefore solubility should increase with temperature. For many cases, however, interactions between gases and the polymers cause solubility to decrease with increasing temperatures. For most gases, it turns out that more easily condensed gases have higher solubility. When solubility is expressed through

Henry's law (equation 2.1), for certain gas/polymer systems, Henry's law constant follows an Arrhenius behavior with temperature, T:

$$H_w = H_{w0} \exp(-\frac{E_s}{RT}) \tag{2.5}$$

where H_{w0} is Henry's law constant at the reference temperature T_0, E_s is heat of solution of the gas in the melt and R is the universal gas constant.

Solubility increases with pressure and may increase or decrease with temperature. For example, solubility of nitrogen increases in PE and decreases in PS with increasing temperature (Han, 1981). For a number of gases, the logarithm of the experimental Henry's law constant has been shown to correlate linearly with $(T_c/T)^2$, where T_c is the critical temperature of the gas (Stiel and Harnish, 1976; Sato, et al., 1996).

Features in the molecular structure of the polymer which disrupt chain packing increase their free volumes. Therefore polymers with branched structures or bulky pendant groups in their repeat unit have increased solubility, relative to polymers with more linear structures. Specific interactions such as hydrogen-bonds between the gas molecules and the polymer repeat structure can also promote solubility.

Experimental data by Durrill and Griskey (1966, 1969) indicate that Henry's law constants rank as $N_2<CO_2<ClF_3C$ for each polymer from the group of PE, PP, PIB, PS and PMMA. Thus, for these systems comprising non-polar or low polarity polymers, solubility was primarily dependent on the type of gas rather than the type of polymer, with CFC showing much higher solubility than atmospheric gases. From the above data, other

researchers (Park et al., 1997) working on microcellular foaming estimated very similar solubilities of CO_2 at 200°C and 27.6 MPa in various polymers such as PP and PS (12%), (15%) and PMMA (15%). Heat of solution was found to be positive for nitrogen in PE but negative for CO_2 in PE, PP and PS (Han, 1981; Durril and Griskey, 1966). For the PS/CO_2 system, recent data indicate good agreement between theory and experiment with correct prediction of decrease of solubility with increasing temperature (Xie and Simha, 1997).

For amorphous polymers without strong polar groups, the linear relation between log-solubility and critical temperature or boiling point of gas (Stiel and Harnish, 1976) may be used as a first approximation. For polybutadiene, for example, solubility of gases decreases with decreasing critical temperature in the order CO_2>CH_4>Ar>N_2 (Sato et al., 1996), with positive temperature dependence for N_2 and negative for CO_2, CH_4 and Ar. However, for amorphous polymers with strong polar groups, significant effects of the polarity of the polymer on gas solubility have been observed (Van Krevelen, 1976; Berens and Huvard, 1989). For example, the solubility of CO_2 at 25°C in butadiene/acrylonitrile rubber increases with increasing content of acylonitrile polar groups in the polymer, whereas that of nitrogen, hydrogen and oxygen, (being already much lower than CO_2 by an order of magnitude), decreases (Van Krevelen, 1976). Equilibrium uptakes of CO_2 at room temperature range from 3% in PE, to 27% in PMMA to over 50% in PVAc. Equilibrium sorption of CO_2 in styrene/acrylonitrile copolymers increases with AN content and in ethylene/vinyl acetate with increasing vinyl acetate monomer. For a variety of polar polymers, solubility of CO_2 ranks as EVA>PMMA>PC>PVC (Berens and Huvard, 1989). The relatively high sorption values of CO_2 in polar polymers may result from enhanced

specific interactions of CO_2 with carbonyl or nitrile groups; these could be related to its quadrupole moment or its H-bonding basicity (Berens and Huvard, 1989). Recent work (Elkovitch et al., 1998; 1999; Lee et al, 1998; 1999) on melt mixed PS/PMMA blends demonstrated that the solubility of CO_2 in the PMMA phase is, indeed, significantly higher than that in PS. Higher affinity with the carbonyl group of the PMMA polymer implies also higher plasticization capacity which is manifested in lower T_g (Wissinger and Paulaitis, 1991) and lower viscosity.

2.2.2 Measurement of Gas Solubility

Many research efforts have been devoted to the subject of gas solubility in polymer melts in the past fifty years. Newitt and Weale (1948) studied the dissolution and diffusion of hydrogen, nitrogen, carbon dioxide, and ethylene in polystyrene. They used sorption experiments and diffusivity measurements by movement of a color boundary. Their data showed that Henry's law is applicable for the systems they studied (nitrogen, hydrogen with polystyrene) for pressures up to 300 atm. Similar sorption experiments were performed by Lundberg et al. (1963). They used the simple sorption technique combined with an automated data log system, and found that Henry's law held to at least 100 atm for systems of nitrogen or methane with polyethylene. Durrill and Griskey (1966; 1969) modified the technique and determined solubilities and diffusivities of various gases (helium, nitrogen, carbon dioxide and argon) in molten or thermally softened polymers (polyethylene, polyisobutylene, polypropylene). They also determined solubilities of the preceding gases in polystyrene and polymethylmethacrylate for pressures up to 20 atm. Henry's law was found to hold up to the pressures they studied. They also attempted to

extend the correlation developed by Micheals et al. (1963a) for solubilities and diffusivities (Michaels et al., 1963 b) of gases in solid polymer systems and found those correlations to be inapplicable for molten and thermally softened polymers. Durrill and Griskey (1969) correlated solubilities and diffusivities of gases in molten or thermally softened polymers with structural characteristics, temperature, and pressure. They obtained Arrhenius type temperature dependence for both Henry's law constants and diffusivities. No appreciable effect of pressure was found for either Henry's law constants or diffusivities up to 300 atm. They developed generalized correlation for diffusivity by relating it to gas Lennard-Jones collision diameter or molecular diameter. A close examination of their results shows that while the diffusivity is a strong function of temperature, the temperature dependence of gas solubility is weak.

All the above investigators conducted high-pressure sorption experiments in which solubility and diffusivity data were simultaneously obtained. The sorption experiments were carried out with measurements of pressure decreasing with time as gas was sorbed into a polymer solution at constant temperature. Solubilities and diffusivities were then estimated by fitting an appropriate diffusion equation to a transformation of the experimental data. This technique is generally referred to as the pressure decay method, and till today, it is still being considered to be one of the most reliable methods used for solubility measurements. But performing such experiment is time-consuming and requires proper preheat of gas (Durrill and Griskey, 1966) and careful calibration.

Duda and Vrentas (1968) obtained solubilities and diffusivities for n-pentane in polystyrene at 1 atm and 413 to 443K by the use of a quartz spring sorption apparatus. Similar measurements were made by Duda et al. (1973) for ethylbenzene in polystyrene

for the temperatures from 433 to 451K and approximately 1 atm. This technique can only be used for measuring solubility under low pressures.

Another major technique used in the past to determine solubility of gases in polymers is the gas chromatographic technique. In this technique, the column is normally coated with polymer, solutes are injected into the carrier gas (normally helium) and then passed through the column; solubility data can be obtained by relating the retention time with the amount of solute absorbed. Chromatographic measurements of solubilities in molten polystyrene at low pressures were obtained by Brockmerier et al. (1972) for benzene and ethylenebenzene at 120°C and ethylbenzene at 180°C. Maloney and Prausnitz (1976) used this technique to obtain solubility (Henry's law constants) of ethylene and other organic solutes in fluid low-density polyethylene in the region 124°C to 300 °C. Using a similar technique, Stiel and Harnish (1976) measured solubility of sixteen organic solutes in molten polystyrene for temperatures from 135 °C to 230 °C and pressures to 4 atm. The Henry's law constants obtained from their study along with those obtained by other investigators were related to the reduced temperature, namely, a linear relationship between the log of the Henry's law constant and $(T_C/T)^2$ as follows:

$$\ln(1/K_P)=-2.338 + 2.706(T_C/T)^2 \qquad (2.6)$$

where K_P is Henry's law constant, T is the system temperature, and T_C is the critical temperature of the solute. They found that this relationship is applicable for systems with $(T_C/T)>0.6$ for all systems they incorporated.

The gas chromatographic technique is normally used to measure solubility of organic solutes (which have high solubility in molten polymers) under low pressures.

Dey (1990) measured solubility of N_2 in PE for pressures up to 200 atm under different temperatures using a steel high-pressure vessel. Dagli et al. (1989) developed an apparatus, a high-pressure chamber, to measure gas solubility of nitrogen in polyolefins. They also related extruded foam properties to the solubility of the specific gas in the polymer melt.

A gravimetric method employing an electrobalance was also used by some investigators to measure gas solubility in polymers (Kamiya et al., 1986). More recent work utilizing this method has been done at the National Research Council of Canada. Researchers measured solubilities and diffusivities of CO_2 in polystyrene and in PVC at 35°C (Wong and Handa, 1997), and their results showed good agreement with literature data obtained using the pressure decay method. Solubilities of blowing agents HCFC142B, HFC134A, HFC125 and isopropanol in polystyrene at 120°C were also measured using this technique (Daigneault et al., 1997). Their results show that in order of decreasing solubility, the blowing agents rank: isopropanol > HCFC142b > HFC134a >HFC125. Solubilities for the same systems were also obtained by the same researchers by measuring vapor-liquid phase equilibria using a high pressure vessel. Much difference in the data acquired by the two methods was observed, especially for the HFC134a – PS system (Daigneault, et. al., 1997). The researchers attributed the difference to the error-prone process of calibration required for the microbalance system under high temperature. The effect of shear on the blowing agent solubility was also studied by varying the mixing

rpm in a high pressure vessel; it was found that introducing mixing somewhat lowers the blowing agent solubility (Caron, et al., 1997).

The major drawback of this gravimetric method, aside from its requirement for a delicate microbalance that requires careful calibration, is that the measurement temperature is very limited. The technique described by Daigneault et al. (1997) can only go up to 125 °C, which makes this method not suitable for many polymer systems.

On-line methods have drawn attention in recent years. Dual transmission infrared sensors have been used for on-line monitoring of foaming processes, the sensors being linked with fiber-optic cables to a FTIR spectrophotometer which records spectra of the melt in the near-infrared region. Infrared probes were mounted on a slit die to monitor the polymer-gas mixtures during the extrusion of foams (Moulinie et. al., 1998). This technique was also used by the same researchers to detect degassing in the melt. Ultrasonic sensors were also used in the same slit die for measuring the phase behavior of molten polymers. Tsujimura et al. (1998) studied the dynamic behavior of bubble nucleation in a slit die with quartz glass windows using a long-distance microscope and a high-speed video system. The effect of nucleating agents on bubble nucleation dynamics for a PP-butane system was also studied using this method.

2.3 Summary

In view of the literature available, it was found that solubility is a principal parameter needed in designing and controlling/optimizing a foam extrusion process. This is especially important when inert gases, which have very low solubility in polymer melts, are used as alternative physical blowing agents. Solubility, to some extent, dictates the

feasibility/efficiency of a particular foaming process. It plays a significant role in all stages of the foam extrusion process including gas dissolution, bubble nucleation/growth and cell structure stabilization. Moreover, solubility continues to play a role in influencing the long-term thermal and mechanical properties of the foamed products during their storage and usage.

Most of the traditional off-line solubility measurement methods require delicate equipment and careful calibration, which in most cases are error-prone; also, it is very difficult- in some cases not possible-to obtain high temperature data, which makes these methods not suitable for many polymer systems. The in-line method developed in this study is shown to provide a fast and convenient way to measure gas solubility in polymer melts under actual foaming conditions. Bubble dynamics in foam extrusion and relation of solubility with processing conditions can also be readily studied. Data obtained using the in-line method could be used directly to characterize a thermoplastic foaming process.

The in-line method, (which determines solubility by observing the onset of bubble dissolution), when combined with measurements in barrel and gas injection conditions, can be used to study the gas dissolution characteristics inside the extruder. Another main advantage of such method is that effects of polymer modification on gas solubility could be studied directly by integrating the optical system with a reactive extruder.

CHAPTER 3

THE IN-LINE METHOD

The in-line method developed in this study utilizes video microscopy in connection with a single-screw or a twin-screw extruder specially configured for foaming purposes. Metered quantities of polymers and specific gases are blended in the extruder which is capable of producing polymeric foams of various densities. A specially designed optical window and flow restrictor valve placed between the die and the end of extruder are used to generate in-line solubility data by observing the onset of bubble formation/dissolution at the window through a microscope-CCD camera-monitor/recorder system. This system is capable of determining solubility of gases in polymer melts under or near actual foaming conditions. The equipment used, the general operation of the process, the measurement techniques employed and testing of the experimental system are discussed below in detail.

3.1 Equipment

A schematic of the in-line measurement process is given in Figure 3.1. The main segments of the process will be discussed individually.

3.1.1 The Extruder

A 32mm (1.25") diameter Killion segmented single screw extruder with length to diameter ratio of 40:1 was used to carry out the initial experiments. This extruder is specially configured for making polymer foams of various densities. The large L/D ratio is

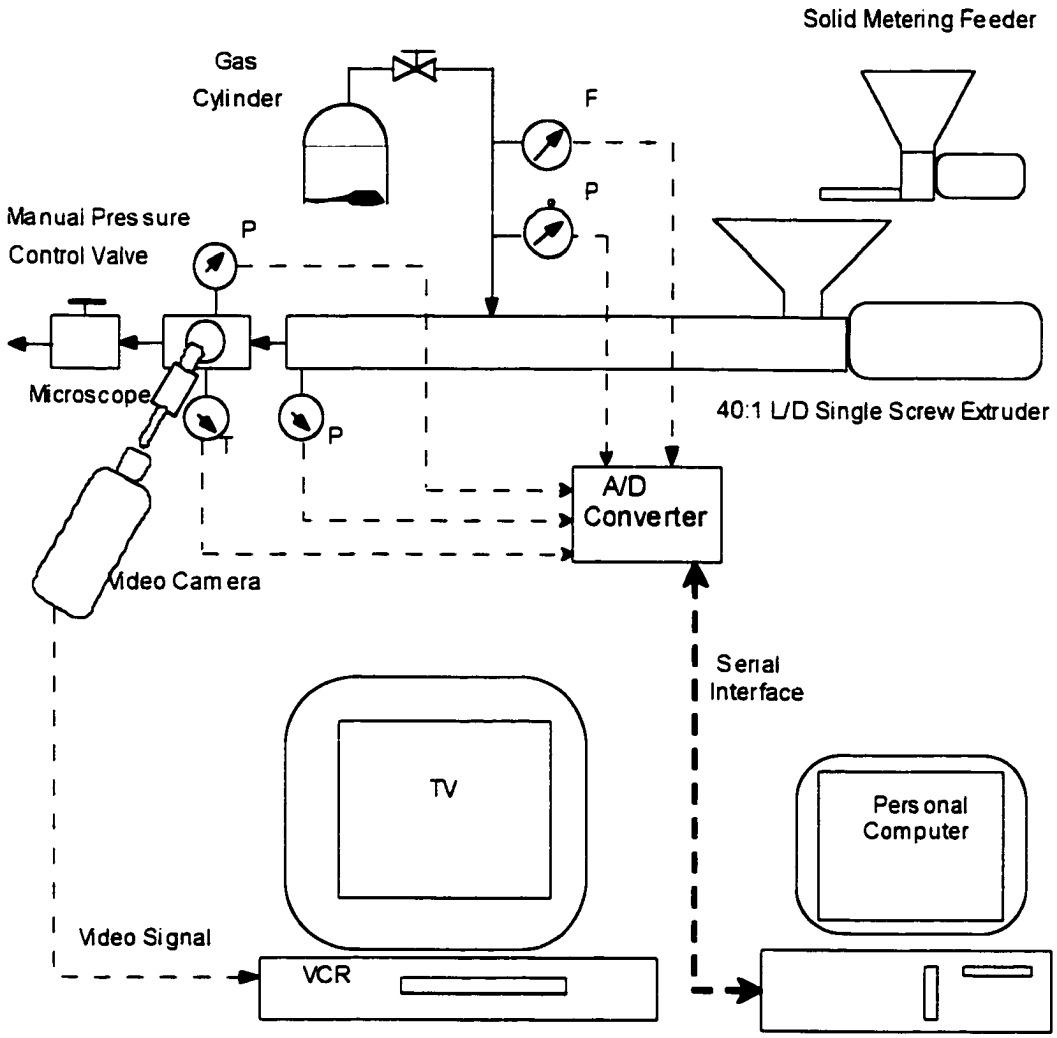

Figure 3.1 Schematic of the Experimental Setup

necessary for purposes of gas injection/dissolution, proper mixing and foaming. A two-stage screw as shown in Figure 3.2 is used for the same purpose. Polymer resin is metered into the extruder using a solid metering feeder and is plasticized in the transition zone within 19D length. The gas (as physical blowing agent) is injected at this point and mixed in the melt. A ring is installed between the two stages of the screw to form a melt seal which prevents gas from flowing toward the back of the system and leaking out of the extruder. Measurement of pressures before and after the injection port ensures that the ring works effectively. A relatively long screw element (about 4 turns) is devoted to gas dissolution. Under normal operating conditions, the degree of fill of this section is low, which provides much volume for the gas to occupy and allows gas diffusion into the polymer melt. The melt-gas mixture is then pressurized in the short compression zone and then mixed and homogenized in the mixing elements that follow before being metered to an optical cell located before the die.

Barrel temperatures are controlled using electrical heaters in nine different zones, which gives the freedom of setting desired temperature profiles.

3.1.2 The Window and Control Systems

The dimensions of the optical cell are shown in Figure 3.3. The specially designed flow cell consists of a rectangular housing with two sapphire windows screwed on both sides of the cell. The cell is heated with four cartridge heaters. A pressure transducer is installed on the window to measure the melt pressure at that point. A retractable thermocouple is

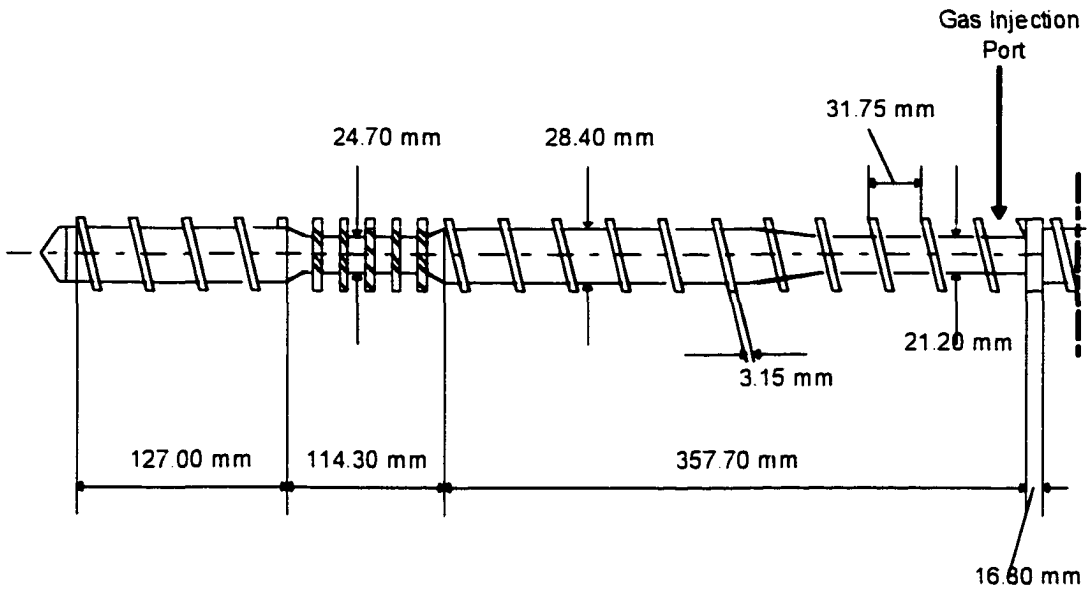

Figure 3.2 Schematic of the Screw Configuration of the Single-screw Extruder (Showing the 2nd Half of the Screw)

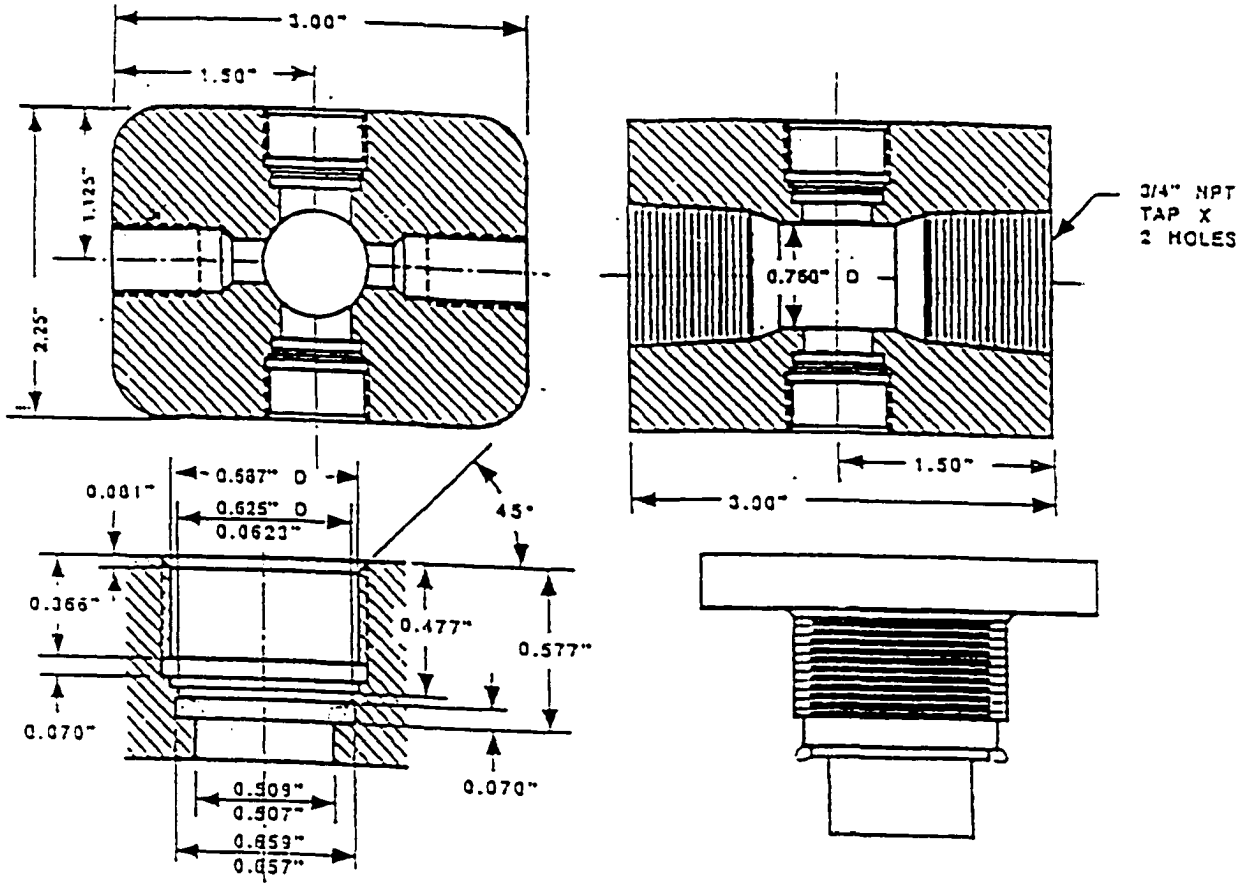

Figure 3.3 Dimensions of the Optical Cell

also installed which enables measurement of the melt temperatures at different vertical locations inside the window.

A manually operated valve is installed after the cell for independent control of the melt pressure at the cell. This valve is also specially designed to offer accurate and fine control of the melt pressure at the window in a wide pressure range.

3.1.3 The Monitoring/Recording System

The monitoring/recording system consists of a standard microscope, a CCD (charge coupled device) video camera, a monitor and a recorder. The microscope/camera is mounted on a traveling device to allow easy focusing. Figure 3.4 shows the schematic of the optical window-monitoring/recording system.

The microscope utilized in this experiment is a regular standard microscope. The primary magnification of a microscope is determined by the magnification specified for the objective and the eyepiece. For a standard microscope:

$$\text{Primary Magnification} = \text{Objective} \times \text{Eyepiece} \tag{3.1}$$

After specific lenses (objective and eyepiece) are chosen for a specific tube length, the primary magnification is fixed; this also determines the field of view, which is defined as the area of the object that will be viewed on the monitor. The CCD camera takes the image and places it on the whole screen of the monitor, so the overall magnification is proportional to the monitor screen size. The overall magnification can be calculated by:

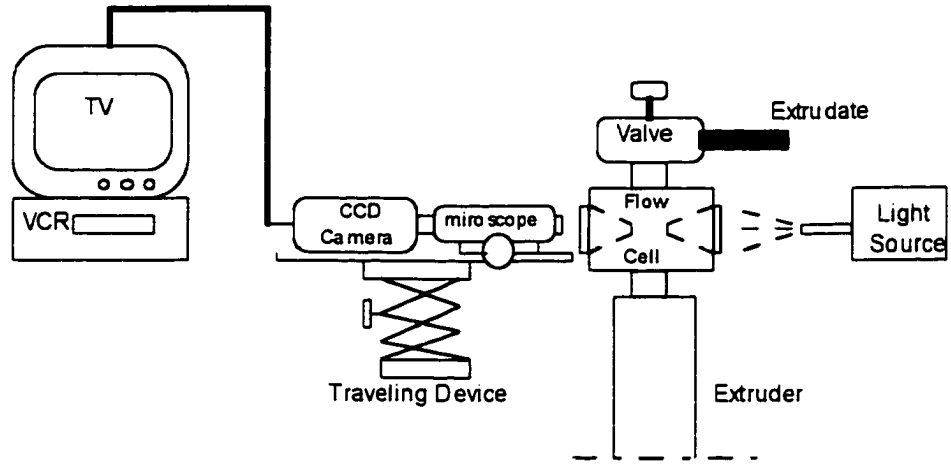

Figure 3.4 Schematic of the Flow Cell-Monitoring/Recording System

Overall Magnification = Monitor Screen Size/Field of View (3.2)

A SANYO CCD camera is used in this study. Different sized monitors are used, and a four-head VCR is used as the recorder.

This system can achieve an overall magnification ranging from 40 to 200 times by selectively using different lenses/monitor combinations. Microscope body extension tubes are also available to increase the overall magnification.

3.2 Instrumentation and Process Measurements

The important process parameters such as melt temperature and pressure at the die and the window, the gas pressure and flow rate are digitized using Keithley Metrabyte's modules. The modules are connected to a serial port of an IBM PS2 computer. A previously developed program is used to achieve real time data acquisition. The parameters are monitored by the computer and also saved in files for off-line analysis.

The polymer throughput is calibrated in two different ways. First, the volumetric feeder is calibrated and a flow rate vs. feeder rpm curve is obtained for every material used. Calibrations were also done for the extrudate for each run before the gas is injected; these procedures served as tests on the flow consistency.

A very important parameter of the process is the gas flow rate. A MKS 2258A-500RK mass flow meter with a type 246B readout is used to monitor the gas flow rate. The flow rate data are also digitized and saved in files for off-line analysis.

3.3 Experimental Procedures

For each experiment, polymer resin is metered into the extruder using a solid metering feeder, it is plasticized and the flow is considered to be fully developed in the first half of the two-stage screw (within 19D length). The gas (physical blowing agent) is injected at this point and mixed/dissolved in the melt; the melt-gas mixture is then pressurized and metered to the optical cell located before the die. The pressure at the window is controlled by carefully adjusting the manually operated control valve.

The presence or absence of gas bubbles in the melt is monitored using the microscope - CCD camera - TV/VCR system. As shown in Figure 3.4, the microscope/camera is mounted on a traveling device to allow easy and accurate focusing. During the experiment, different combinations of lenses are normally used because sometimes it is necessary to use low magnification for larger field of view while quite often the highest magnification is required.

Figure 3.5 shows the images taken from a test run for a polystyrene (PS)-CO_2 system. They illustrate how the procedure progresses. In the early stages of the experiment, when the window pressure is low, a large number of large bubbles exist in the melt as shown in Figure 3.5(a). The system can be viewed as a two-phase system consisting of a continuous melt phase and a dispersed bubble phase; the window pressure is then slowly increased by adjusting (closing) the restricting valve. The number and the size of the bubbles decreased with increasing melt pressure. Figure 3.5(b) shows this tendency when pressure was elevated but still not reaching the point where all gas is dissolved in the melt. When the pressure reached a certain point, all bubbles disappear and the system appears to be a single-phase system as shown in Figure 3.5(c); this pressure is

considered to be the lowest pressure required to keep all the gas in solution under the specified conditions. Combining all the information with the gas flow rate and the melt throughput, solubility can then be calculated.

In order to ensure accuracy, great care must be taken during the experiment. In each experiment, the window pressure should be increased very slowly while carefully observing the bubble dynamics. When the system reaches a stage such as that shown in Figure 3.5(b), one should wait long enough (typically 30 to 40 minutes) to allow the system to stabilize and then record this pressure. The window pressure may then be slowly increased to make all bubbles disappear and kept long enough under this new condition to allow the system to stabilize and also record this pressure. A pressure range is established in this way. The target pressure, being somewhere in between, is determined by decreasing the window pressure to allow the bubbles to re-appear and stabilize the system, re-starting the above process and trying to narrow the gap of the pressure range to a significantly small number so that the accuracy is ensured.

Gas flow rates are obtained by taking average values based on the recorder output. Due to the dynamic nature of the process, fluctuation of the gas flow rate will exist throughout each experiment and this may contribute to possible errors.

3.4 Observation of the Bubble Dynamics

The essence of the method is to find the saturation pressure for the system under specific conditions by observing the onset of bubble formation/disappearance. So the two major concerns regarding the accuracy of the method are: a) how fast the bubbles travel through the window and, b), what is the smallest bubble size that can be clearly viewed through the

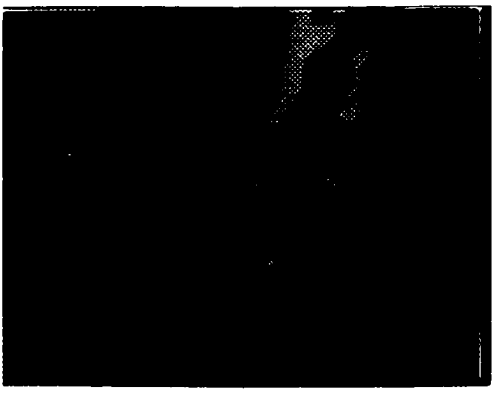

a. Low Pressure

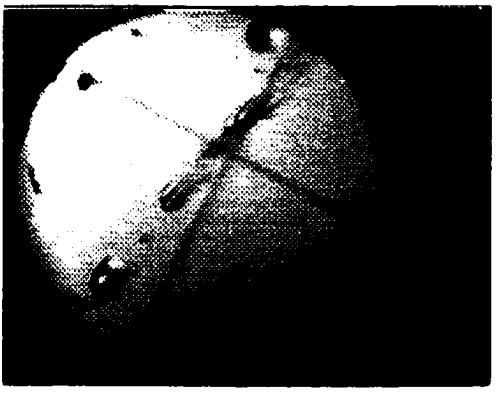

b. Pressure Close to the Targeted Pressure

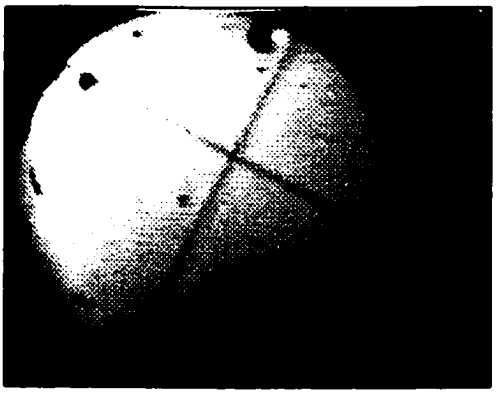

c. High Pressure

Figure 3.5 Monitoring of CO_2 Bubbles in PS Melt at 215°C (6

optical setup. If bubbles flow very quickly through the window, it will be difficult to observe/record the bubble dynamics, hence causing experimental error. The actual experiments showed, however, that this is not a concern. A very interesting observation during the experiment is that when system pressure was far below the actual saturation pressure, bubbles existed everywhere in the melt with greater concentration near the window wall as shown in Figure 3.6a. When the pressure was increased to the close vicinity of the actual saturation pressure, it was observed that bubbles existed only near the window wall, as shown in Figure 3.6b and 3.6c. These bubbles travel with the melt at a very slow speed near the window wall surface. The average velocity of the bubbles shown in Figure 3.6c is 0.0025cm/s while the corresponding average melt velocity is 0.13 cm/s. Another example with much higher melt velocity is shown in Figure 3.7, where bubbles flow at 0.008cm/s while the average melt velocity is 0.40 cm/s. This also gives time for the bubbles to grow, hence allowing better observation.

Although this procedure involves bubble nucleation and growth, it is quite different from an actual foaming process. It has been shown that for large-scale simultaneous bubble nucleation to occur, a high to modest degree of supersaturation and shear must both be present (Lee, 1993). A foaming process meets this standard because nucleation happens near the die exit where highly supersaturated gas-laden melt flows out of the die under high shear. In the solubility measurement procedure, pressure is intentionally adjusted very close to the saturation pressure, i.e., the degree of super-saturation is low. The type of nucleation that normally happens during the foaming process does not occur, since only a very small number of bubbles nucleate on or near the wall of the flow channel where shear rate is high. This is consistent with the generally recognized theory that shear

promotes nucleation (Lee, 1993). The roughness of the wall might also have served as a nucleating site that promotes bubble nucleation. Bubble nucleation is generally considered to be a heterogeneous process although self-nucleation may occur at high supersaturation (Han, 1981). Impurities in the melt can also serve as nucleating agents to assist bubble nucleation. The fact that only very small amount of bubbles nucleate under near saturation conditions significantly enhances the accuracy of the in-line method, since sufficient amount of gas is available for those nucleated bubbles to grow, even though the overall degree of supersaturation is very low (near saturation).

The bubbles observed in the window area during the experiment are actually nucleated somewhere upstream and underwent some degree of initial growth. The rate of bubble growth relative to the degree of supersaturation dictates the sensitivity of the method. Regular TV, the monitor used in this study, is generally regarded having poor resolution, and can not clearly view bubbles with diameters below 5mm on the screen; this corresponds to 25 μm at 200X magnification. The situation is further complicated by the impurities present in the commercial resins used. Bubbles can be distinguished from impurities since bubbles have well defined shapes while impurities tend to be irregular in shape and size. Also, bubbles change size (grow/shrink or combine/divide) during flow while impurities normally remain unchanged.

Figure 3.6 [n-[

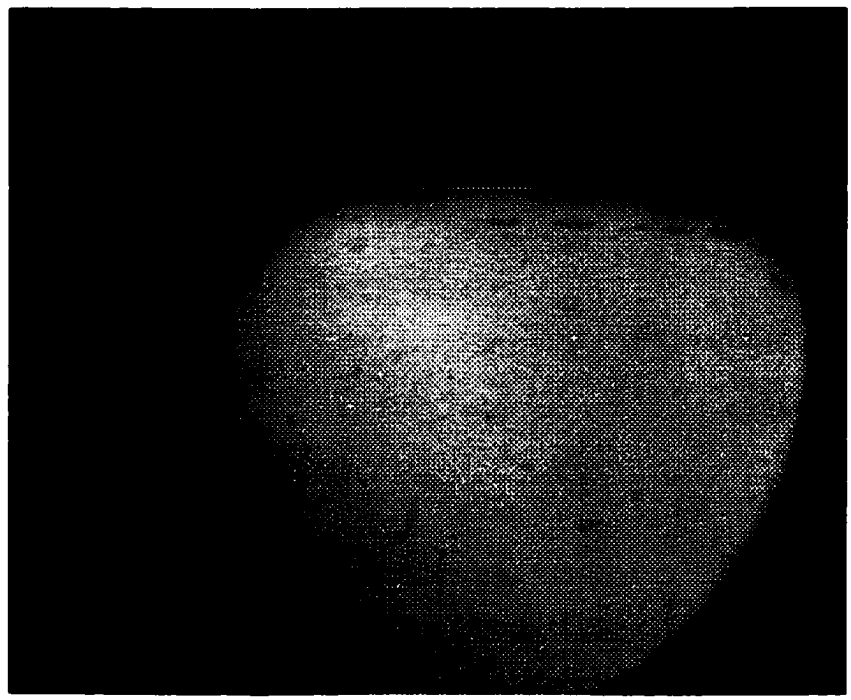

Figure 3.7 In-Line Monitoring of CO_2 Bubbles in PS Melt at 215°C (100X)

Classical bubble growth studies have shown that after bubbles are nucleated, they undergo rapid initial growth. Bubbles grow against the viscous media driven by the pressure difference between the saturation pressure and the ambient. In the present case, however, the driving force is very small due to the low degree of supersaturation.

Research has shown that nucleation starts with a nucleating site in form of clusters. Whether a cluster begins to grow into a bubble depends on a pressure differential between the gas inside the microbubble and the gas-laden melt surrounding it and the nucleant. This is described by the first Rayleigh equation (Levitskiy and Shulman, 1995):

$$P_{inside} \geq P_{melt} + 2\sigma / r \tag{3.3}$$

where σ is the surface tension. Until recently, it was assumed that for most polymers, the surface tension was approximately 30 dyn/cm, a typical value for most organic liquids (Throne, 1996). Some researchers claim that the surface tension for certain polymer-gas systems can be substantially lower than this value, perhaps as low as 5 dyn/cm (Throne, 1996). More importantly, the surface tension may be strongly affected by the nature of the dissolved gas and the presence of any processing aids at the bubble-gas-laden melt interface. When the gas-laden melt is depressurized during foaming or in the solubility measurement process, once the pressure has fallen below the saturation pressure of the gas in the melt, nucleation begins and the bubble begin to grow from its critical radius r. From polystyrene-toluene experiments, Han and Han reported a critical bubble radius of 0.3 μm (Han and Han, 1990). Other researchers' calculations have shown that under practical

extrusion foaming conditions, stable bubbles can only come to existence from their nucleation sites when their size reaches 40-50 μm for most polymer-gas systems (Dey, 1998)

It is now generally accepted that the fluid resistance to incipient bubble expansion is shear viscosity. This is described by the second Rayleigh equation which is obtained by combining the momentum and continuity equations around an expanding sphere (Throne, 1996). It includes the shear stress, τ_{rr} at the interface between the expanding gas and the melt:

$$P_{gas} = P_{melt} + 2\sigma / r - \tau_{rr} = P_{melt} + 2\sigma / r + 4\eta_0 \dot{r} / r \qquad (3.4)$$

Where η_0 is zero-shear viscosity, and $\dot{r} = dr / d\theta$ is bubble growth rate. Rearranging equation 3.4 shows that the bubble growth rate is inversely proportional to the viscosity of the gas-laden melt. Polymer viscosity is strongly dependent on temperature. Furthermore, the viscosity of the gas-laden melt is a strong function of the polymer-gas mixture and the gas concentration. As the gas concentration increases, the zero-shear viscosity decreases and the bubble will grow more rapidly.

It is observed during this study that even when the degree of supersaturation is very low, under normal flow conditions, bubbles grow rapidly during flow. Figure 3.8 is an example showing this tendency. The actual melt pressure is 1413 kPa while the corresponding saturation pressure is 1461 kPa. Under these conditions, it takes approximately 60 seconds for a bubble to travel through the observed window area;

during this time period, a few hundred times of growth in volume is observed. Figure 3.9 shows the situation when the melt pressure is further decreased for the same system. In this case, due to the relatively high bubble concentration, some bubbles tend to combine with each other while some others, especially those touching the window surface, are divided into smaller ones during flow. Although it is difficult to determine exactly the extent of bubble growth, growth is clearly visible from Figure 3.9. As mentioned earlier, during the solubility measurement, bubbles tend to nucleate and flow near the window surface at low speed, giving time for bubble to grow; this greatly facilitates observation. More importantly, the bubbles nucleated upstream grow to a size clearly visible through the microscope-camera-monitor system in short time when the actual pressure is very close to that of saturation (the pressure in the above example is about 96.7% of the targeted pressure); this further ensures accuracy and sensitivity of the in-line method.

3.5 Testing of the In-Line System - Preliminary Results

The system was tested for an amorphous polymer/inert gas system (Polystyrene-CO_2) for ease of operation and availability of literature data. Numerous modifications have been made during the 11 runs on the PS-CO_2 system.

A general purpose amorphous polystyrene (DOW 685D) was used to carry out this series of test runs. CO_2 was used as physical blowing agent. All the experiments were carried out at a constant temperature of 215 °C. A summary of the experimental results is presented in Table 3.1. A plot of solubility (i.e., cm^3 [STP] gas dissolved/g-melt) vs. melt pressure for the system is given in Figure 3.10. The first set of data shown in the Figure were obtained in the earliest experiments where the CO_2 flow rate was recorded using a Sargent Welch recorder (Model XKR). Due to the fluctuation of the flow rate, the accuracy of the average flow rate was not very good. The second data set was obtained after the system was modified by digitizing the gas flow rate into computer files for off-line analysis; the error on flow rate was reduced. Another difference between these two sets of data is that the second set of was obtained at a slightly higher polymer flow rate. A linear regression on all data points by forcing the line pass through the origin is presented in Figure 3.11. A solubility value of 0.0027 cm^3[STP]/g•kPa with R^2=0.9459 is obtained from these results. The data indicate that linear behavior is followed over the pressure range studied. However, the data points at low pressure are substantially off the solubility curve, resulting in deviation of the regression line from the origin. This will be further studied in the following experiments.

Table 3.1 Summary of Experimental Results for the Polystyrene - CO_2 System (Melt Temperature: 215 °C, Screw rpm 15, Feeder rpm 15/20)

Run No.	Gas Flow Rate (cc[STP]/min)	Melt Flow Rate (g/hr)	Solubility (cc[STP]/g Melt)	Melt Pressure (kPa)
1	30.0	971.4	1.85	1630.3
2	35.0	976.1	2.15	1711.4
3	80.0	886.2	5.42	2738.8
4	90.0	886.2	6.10	3382.2
5	160.0	969.0	9.91	4213.1
6	175.0	969.0	10.84	4319.5
7	230.0	969.0	14.24	5521.2
8	44.5	1350.0	1.98	1345.6
9	103.6	1290.0	4.82	2171.4
10	153.1	1290.0	7.12	2777.3
11	204.6	1350.0	9.09	3411.6

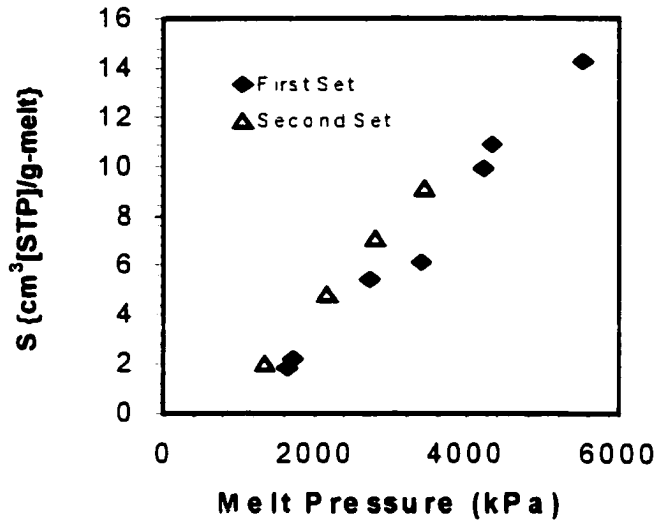

Figure 3.10 Solubility of CO_2 in PS Melt at 215 °C–Comparison of Two Sets of Data Obtained under Different Conditions

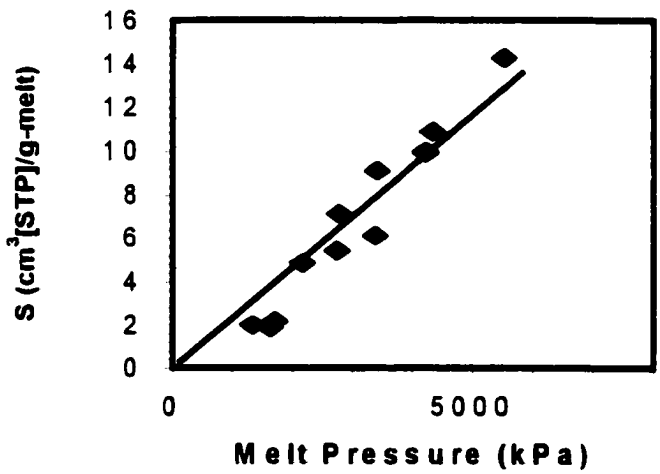

Figure 3.11 Solubility of CO_2 in PS Melt at 215 °C–Linear Regression of All Data Points Shown in Figure 3.10

Assuming the vapor pressure P in Henry's law can be replaced by the melt pressure in this case, the results in Figure 3.11 show that the solubility of CO_2 in PS follows Henry's law. Investigators have found that Henry's law holds up to certain pressures for PS-CO_2 system in batch processes (Durrill and Griskey, 1966; Rein et. al., 1990) where the gas-polymer melt equilibrium could be described by Henry's law.

A comparison of results from these experiments with literature data is presented in Table 3.2. The data obtained from this study compare favorably with those obtained from off-line sorption experiments. It should be noted that the literature results from Durrill and Griskey (1966) were obtained at a slightly lower temperature than that from this work; while the data by Rein et al. (1990) were obtained at a temperature below the polymer T_g. It has been reported by the above authors that solubility of this system decreases with increasing temperature.

3.6 Summary

The experimental results on bubble dynamics have shown that bubbles can nucleate under near saturation pressures; when the degree of supersaturation is very low, the bubbles nucleate only near the window surface where the shear rate is high, which confirms that shear enhances bubble nucleation.

Under near saturation conditions, only a very small amount of bubbles will be nucleated, and, these bubbles undergo rapid initial growth to a size clearly visible by the optical system used in the present study. All of these contribute to ensuring accuracy of the in-line solubility measurement method.

Table 3.2 Comparison of Experimental Results with Literature Data

	Temperature (°C)	H/Slope cm^3 [STP]/g•kPa	Pressure Range (kPa)
In-line data	215	0.0027	Up to 5575
Sorption experiment results (Durrill and Griskey, 1966)	188	0.0022	Up to 2030
Data from low temperature experiments (Rein et al., 1990)	90	0.0039	101.3

The preliminary results show that the solubility of CO_2 in PS increases linearly with pressure. The results are good in agreement with literature results obtained from off-line measurements for the same system.

CHAPTER 4

SOLUBILITY RESULTS FOR TWO POLYMER SYSTEMS

After its feasibility was demonstrated, this in-line method is used to measure solubility data for systems involving inert gases CO_2, N_2, and Ar in polystyrene (PS), an amorphous polymer and in polyethylene terephthalate (PET), a semicrystalline polymer. Temperature effects on solubility of these systems are also studied.

To the author's knowledge, there are no published solubility data available for systems involving these three gases in molten PET. Some limited data are available for these systems obtained at temperatures below the polymer T_g. This is, mainly, because high temperature experiments are very difficult to conduct with conventional methods.

4.1 Results For Systems PS-CO_2, PS-N_2 and PS-Ar

The material used is a general purpose clear polystyrene (DOW STYRON 685D), the same material as used in the preliminary test runs.

A comparison of solubility of different gases in PS at 215°C is given in Figure 4.1. Temperature effects on solubility for systems PS-CO_2 and PS-N_2 are presented in Figures 4.2 and 4.3 respectively. The regression lines in these figures were obtained by forcing the lines pass through the origin. The results show clearly the difference of solubility of different gases in PS. Solubility of all three gases increases linearly with pressure. In decreasing order of solubility, the gases rank CO_2>Ar>N_2. For carbon dioxide, the solubility decreases with increasing temperature. This tendency has been generally observed in many gas-polymer and solute-solvent systems (Han, 1981; Durrill and

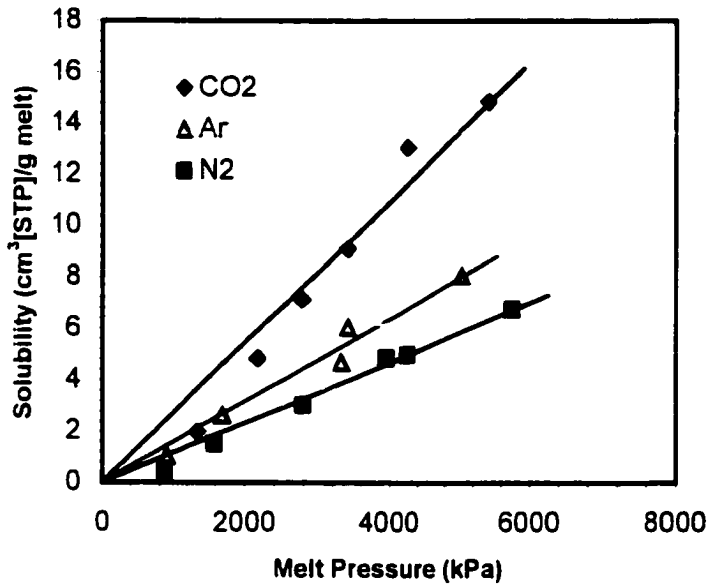

Figure 4.1 Solubility of Gases in Polystyrene Melt at 215 °C

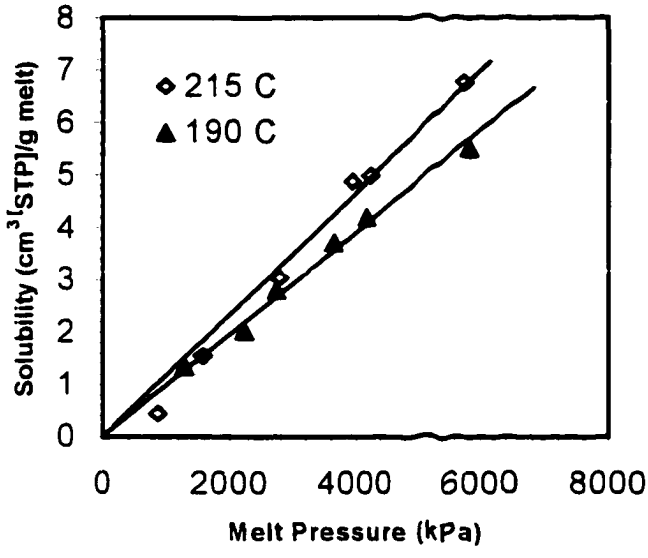

Figure 4.2 Solubility of CO_2 in PS Melt at Two Different Temperatures

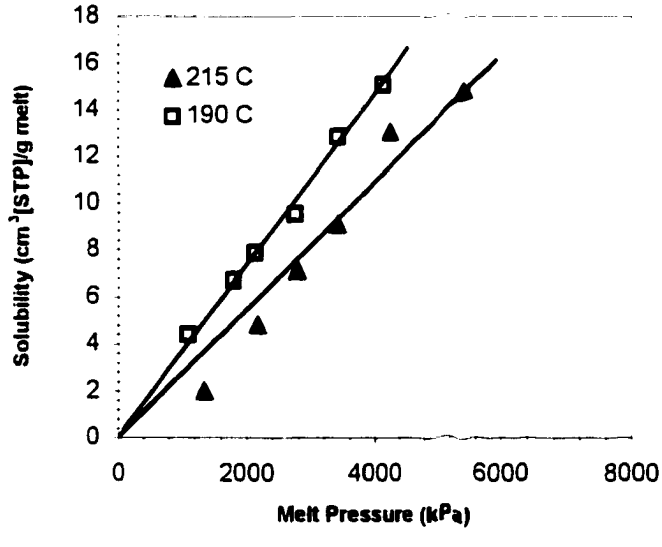

Figure 4.3 Solubility of N_2 in PS Melt at Two Different Temperatures

Griskey, 1966; Sato et. al, 1996). For nitrogen, however, the solubility increases with increasing temperature. This tendency is called reverse solubility and has been observed for gases of low critical temperatures such as helium, hydrogen, nitrogen and oxygen (Sato et. al, 1996). The temperature effect is quite pronounced for both carbon dioxide and nitrogen considering the relatively small temperature range studied.

Sato and co-workers (1996) recently conducted pressure decay experiments and obtained solubility of carbon dioxide and nitrogen in polystyrene at different temperatures. They obtained temperature dependence by correlating Henry's law constant with $(T_c/T)^2$ of the gases involved. The temperature dependence found in this study is more pronounced than that calculated from their equations for both carbon dioxide and nitrogen. A numerical comparison is presented in table 4.1.

It should be noted that in the in-line method, thermal homogeneity of the gas-laden melt in the window area is normally not ideal. A 5-8°C difference in melt temperature between the window wall area and the center was observed during the experiments. As a result, it is likely that the temperature effects shown in Figures 4.2 and 4.3 are somewhat exaggerated.

Table 4.1 Comparison of Temperature Dependence of CO_2 and N_2 in PS (Temperature increasing from 190°C to 215°C)

	CO_2	N_2
This Study	20.5% Decrease	20% Increase
Calculated from Correlation by Sato et. al (1996)	10% Decrease	7.5% Increase

4.2 Results for Systems PET-CO_2, PET-N_2 and PET-Ar

The polymer used in this part of the study is a commercial polyethylene terephthalate (Shell Traytuff 9506 PET) with a nominal IV of 0.95. The PET resin is dried at 120°C in a vacuum oven for about 20 hours prior to each experiment.

Solubility vs. pressure for these systems is shown in Figure 4.4. Results for solubility of CO_2 and Ar at different temperatures are given in Figures 4.5 and 4.6 respectively. Again, the regression lines were forced through the origin in these figures. Similarly to the case of polystyrene, carbon dioxide has the highest solubility in PET, nitrogen has the lowest, and Ar somewhere in between. This trend is consistent with literature results obtained for the same systems under temperatures below the polymer T_g (Micheals et. al., 1963a). Figures 4.5 and 4.6 show that solubility decreases with increasing temperature for both carbon dioxide and argon. While the effect is very small for PET-Ar, the effect is much more pronounced for the PET-CO_2 system. This tendency is also consistent with experimental results obtained using off-line methods under temperatures below the polymer T_g (Faridi, 1998).

4.3 Summary

Solubility of CO_2, Ar and N_2 in two different polymer systems has been obtained using the in-line method developed in this study in a single screw extruder. Temperature effects on solubility of these gases have also been studied and showed similar trends with literature findings. To the author's knowledge, results obtained in this study on solubility of these gases in molten polyethylene terephthalate are the first reported data on this system.

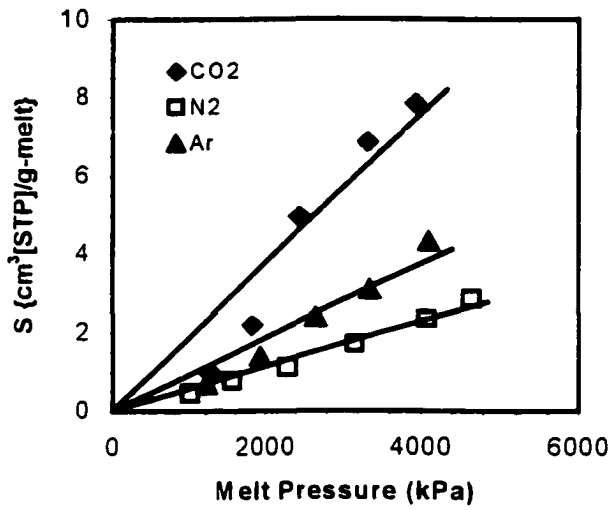

Figure 4.4 Solubility of Inert Gases in PET at 290°C

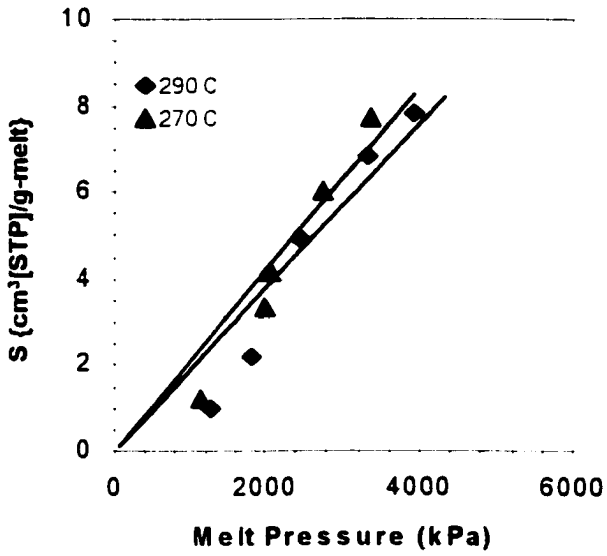

Figure 4.5 Solubility of CO_2 in PET Melt at Two Different Temperatures

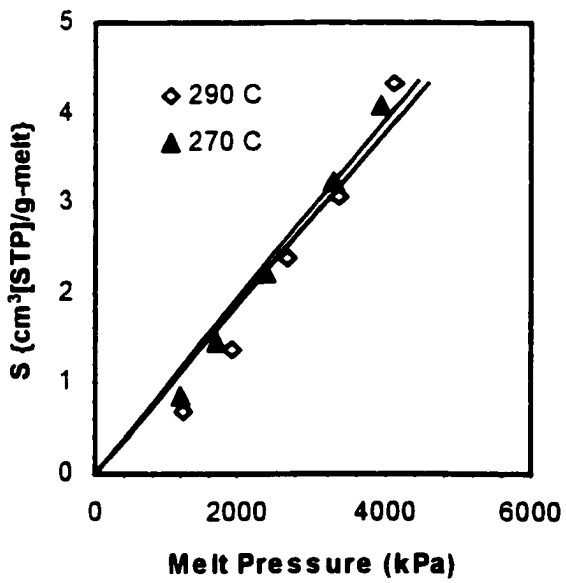

Figure 4.6 Solubility of Ar in PET Melt at Two Different Temperatures

CHAPTER 5

GAS DISSOLUTION DURING FOAMING IN A SINGLE SCREW EXTRUDER

The dynamics of gas dissolution in polymer melts during foaming is an important controlling element of the foam extrusion process. Attempts are made here to mathematically model the gas diffusion process and then compare the results with that obtained from downstream measurement at the window area, and try to elucidate possible mechanisms of the gas dissolution process.

5.1 Model Description

A surface renewal model that includes a rotating polymer pool and a barrel film, both under continuous surface renewal, is used in the modeling. A similar model has been used in polymer melt devolatilization by a number of researchers with varied degree of success (Roberts, 1970; Biesenberger and Kessidis, 1982; Collins et. al., 1985; Biesenberger et. al., 1990).

Consider the screw channel cross section shown in Figure 5.1. Following normal practice, the curvature of the unwrapped channel is neglected. For easy visualization, the reference frame is changed, and the screw is assumed to be stationary with the barrel moving.

As shown in figure 5.1, let V_{BX} be the cross channel velocity, so

$$V_{BX} = \pi DN \sin\phi \tag{5.1}$$

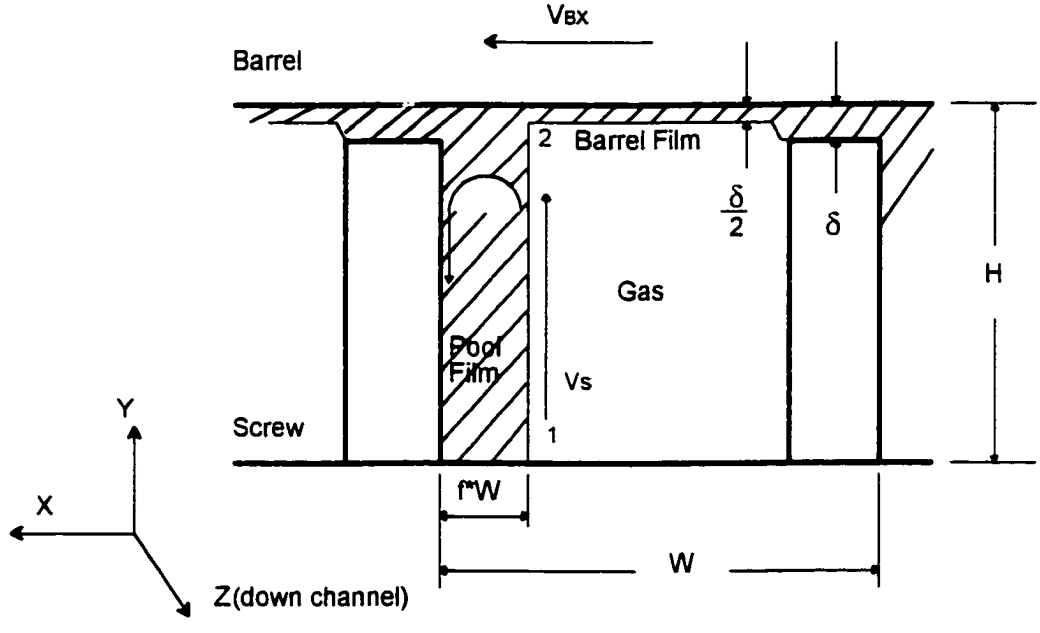

Figure 5.1 Schematic of the Screw Channel Cross Section – Mass Transfer Areas

where D is the barrel diameter, N is the screw speed (rpm), and ϕ is the screw helix angle.

The motion of the barrel causes a circulatory flow (at velocity V_S) of the melt pool that causes a continuous renewal of the free surface from which gas diffuses into the melt. Although the quantitative treatment of this flow is not available, it is reasonable to assume that:

$$V_S = V_{BY} \tag{5.2}$$

An element of polymer at the free surface remains exposed to gas for only a short time, defined here as pool surface exposure time, t_{pe}, which can be estimated by:

$$t_{pe} = \frac{H - \frac{\delta}{2}}{\pi D N \sin\phi} \tag{5.3}$$

where δ is the clearance between the screw flight and the barrel surface.

The model of the system consists of a thin element of polymer moving in the Y direction along the free surface with a velocity V_S. Once this element reaches the point 2 shown in Figure 5.1, the gas dissolution process stops, and the element is mixed into the bulk of the polymer pool. It is assumed that each new element reaching point 1 contains gas at the same concentration as the bulk of the melt pool.

Another mechanism is that the barrel drags a thin film of polymer through the clearance δ between the screw flights and the barrel. The velocity of the polymer is V_{BY} at

the barrel surface and decreases linearly to zero at the tip of the flight if Couette flow is assumed. Once the polymer passes the flight, the velocity gradient disappears, so the thickness of the film reduces to half of its original value as required by continuity. For the analysis, the barrel film thickness is assumed to be $\delta/2$ as soon as the polymer melt passes the flight.

The barrel film is exposed to gas for a time t_{be} , the barrel film exposure time, which is given by

$$t_{be} = \frac{W(1-f)}{\pi DN \sin\phi} \tag{5.4}$$

where f is the degree of fill in the mass transfer region shown in Figure 5.1. After this exposure time, the melt is mixed into the polymer in the upstream flight.

When surface renewal is fast enough that only unsteady state mass transfer exists, penetration mass transfer occurs. The penetration model basically assumes the mass transfer films to be semi-infinite slabs in which the uni-directional diffusion can be described by:

$$\frac{\partial c}{\partial t} = D_{AB}\frac{\partial^2 c}{\partial x^2} \tag{5.5}$$

where c is gas concentration (g/cm^3), t is time (s), D_{AB} is the diffusivity of the gas in the polymer melt, and x is the dimension along the diffusion path.

The boundary conditions are:

(1) The interface is at the equilibrium concentration c_e (g/cm^3)

(2) The film concentration is initially homogeneous at c_i, and the concentration at large depth remains at c_i.

The rate of gas dissolution, n (g/s), of an element of area, a, at time t is then

$$\frac{dn}{da} = (c_e - c_i)\sqrt{\frac{D_{AB}}{\pi t}}dt \tag{5.6}$$

The average rate of gas dissolution per unit area, $\bar{n}$, during exposure time, t_e, can be shown to be:

$$\bar{n} = \frac{1}{t_e}\int_0^{t_e}(c_e - c_i)\sqrt{\frac{D_{AB}}{\pi t}}dt$$

$$= 2(c_e - c_i)\sqrt{\frac{D_{AB}}{\pi t_e}} \tag{5.7}$$

where c, weight concentration, can be converted to weight fraction, w, by:

$$c = w\rho \tag{5.8}$$

where ρ is the density of the gas-containing melt.

The average mass flux over the exposure time of the film can be expressed by:

$$\bar{n} = 2\rho(w_e - w_i)\sqrt{\frac{D_{AB}}{\pi t_e}} \tag{5.9}$$

For the above mentioned process to be valid, the following assumptions are made:

1. The flow throughout the gas dissolution section is fully developed and is plug flow in the down channel direction.
2. The various films in any time increment are all at the same concentration.
3. The mixture is rehomogenized at each film regeneration by the cross channel and flight clearance leakage and through molecular diffusion.
4. The curvature of the free surface of the rotating pool is neglected.
5. The entire gas dissolution section is isothermal.

Take Δz as an increasing step in the down channel direction which is defined by:

$$\Delta z = \bar{V}_{BZ}\Delta t_e \tag{5.10}$$

where $\bar{V}_{BZ}$ is the average down channel velocity, which, by neglecting the shape factor effect, can be calculated from

$$\bar{V}_{BZ} = \frac{\pi DN\cos\phi}{2} \tag{5.11}$$

The degree of fill can be calculated from:

$$f = \frac{m_p}{\rho \bar{V}_{BZ} HW} \tag{5.12}$$

where m_p is the polymer throughput.

For each time step, there are surface areas from which gas diffusion occurs, these films have the following surface areas:

The melt pool surface, a_{pf}, where the subscript "*pf*" stands for pool film, is given by

$$a_{pf} = (H - \delta/2)\Delta z \tag{5.13}$$

The barrel film surface, a_{bf}, where the subscript "*bf*" stands for barrel film, is calculated from:

$$a_{bf} = W(1-f)\Delta z \tag{5.14}$$

The rate of diffusion is summed over all the areas during that time interval:

$$n_A = 2\rho(w_{eq} - w)\sqrt{\frac{D_{AB}}{\pi t_e}} \tag{5.15}$$

The gas dissolution rate in any one step, m_g, is obtained by:

$$m_g = n_d \sum_i a_i \tag{5.16}$$

This calculation is marched forward with incremental mass balances continuously performed until it reaches the compression zone where the screw is filled and the gas dissolution process ceases.

5.2 Modeling Results For PS-Gas Systems and Discussion

Modeling was performed for systems involving polystyrene and three inert gases, CO_2, Ar and N_2. Figure 5.2 presents some modeling results and their comparison with experimental values for systems PS-CO_2, PS-Ar and PS-N_2. Comparisons for each system in a large pressure range are given in Figures 5.3, 5.4 and 5.5 for systems PS-CO_2, PS-Ar and PS-N_2 respectively. In these figures, three quantities are compared for each system under a particular set of conditions. Namely, the amount of gas in solution as calculated from the model, the actual amount of gas in the melt as measured downstream at the window area, and the amount of gas that could be dissolved in the melt assuming equilibrium is achieved (Henry's law). These results show that the amount of gas dissolved in the system as predicted by the model is much less than the actual amount as measured downstream at the window area. It is highly possible that the polymer melt foams in the gas injection zone when it comes to contact with the gas. Foaming would significantly enhance mass transfer by increasing the areas available for diffusion to occur. Foaming enhanced mass transfer

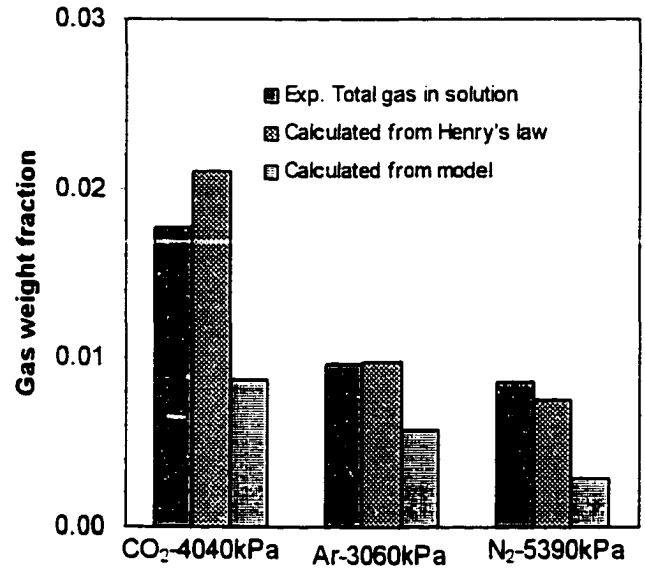

Figure 5.2 Comparison of Modeling Results with Experimental Values (in PS at 215°C)

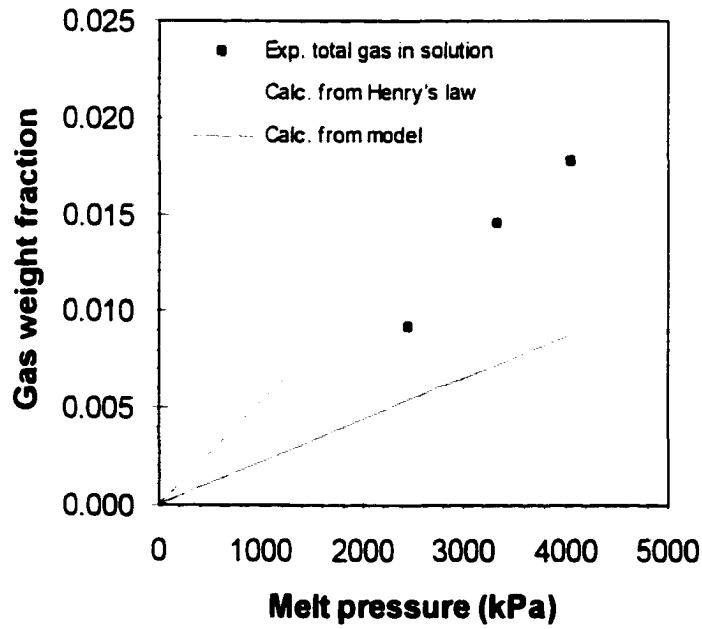

Figure 5.3 Comparison of Gas Dissolution between Model Calculation and Experimental Measurements (CO_2 in PS at 215°C)

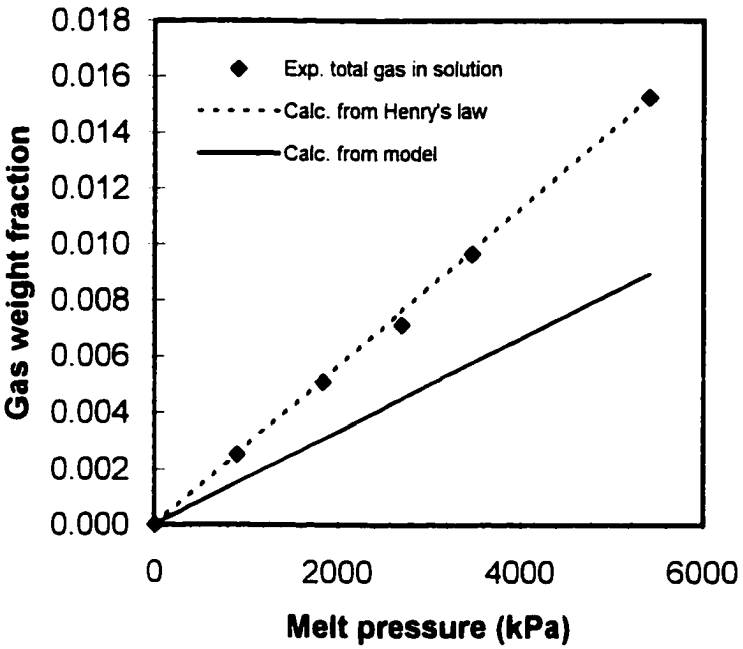

Figure 5.4 Comparison of Gas Dissolution between Model Calculation and Experimental Measurements (Ar in PS at 215°C)

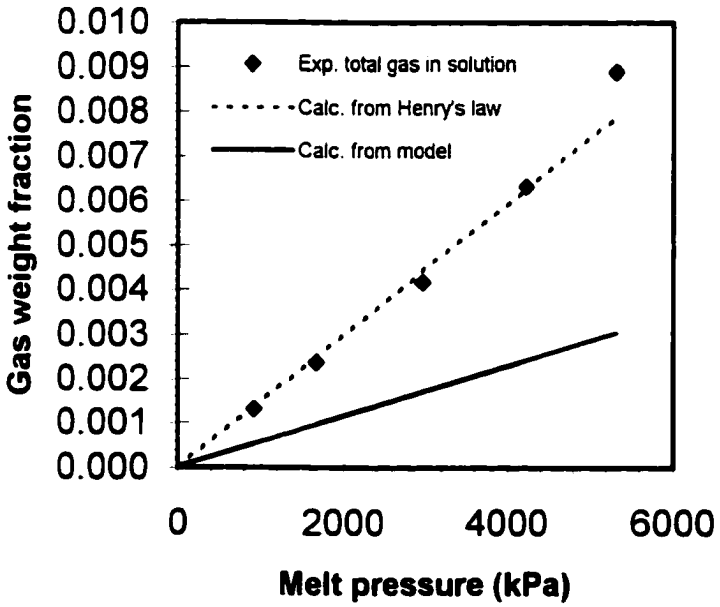

Figure 5.5 Comparison of Gas Dissolution between Model Calculation and Experimental Measurements (N_2 in PS at 215°C)

has been observed and studied by many researchers in polymer devolatilization processes (Biesenberger and Lee, 1986; 1987; Foster and Lindt, 1989; Tukachinsky et al., 1994). It is easy to envision the formation of foam in a devolatilization process where the gas in solution is continuously "bubbling out" of the system under the influence of the vacuum applied to the system. This is essentially a foaming process where the principles of foam formation such as nucleation and bubble growth apply. The gas dissolution process studied here is different from the devolatilization process in that the system is under pressure, so the driving force is positive in the direction of gas dissolution. Todd (1999) observed the formation of bubbles in twin-screw extruders when small amount of air or water is injected into the melt. He also observed that bubbles form in the melt due purely to air entrainment when no gas was injected. The circulatory flow of the rotating melt pool may be capable of trapping some amount of the gas into the melt. This amount of gas can not be readily dissolved into the melt due to the limitations of mass transfer rates, low solubility, diffusivity and short contact time. It can be envisioned that this entrapped gas serves as the source for bubble nucleation and growth, and the degree of foaming continues to grow as the melt flow progresses. It is also possible that certain amount of gas is trapped in the melt in the form of large bubbles. These bubbles break down into many more bubbles with smaller diameters due to the shear stresses applied by the melt, i.e., dispersive mixing. As illustrated by Grace (1982), during dispresive mixing, the size of a dispersed particle breaks down to a critical value defined as R^c, which can be calculated from critical capillary number, C_a^c, defined by:

$$C_a^c = \frac{\dot{\gamma}_m \eta_m R^c}{\sigma} \tag{5.17}$$

where $\dot{\gamma}_m$ is the melt shear rate, η_m is the viscosity of the melt, and σ is surface tension. As shown in Figure 5.6 (Grace, 1982), unique relationships between C_a^c and the ratio of the dispersed phase viscosity η_d to the matrix viscosity η_m exist for each of the following types of flows: shear flows and extensional (stretching) flows. In the rolling melt pool and later on the metering zone of single screw extruders, shear flows prevail. In twin-screw extruder full kneading elements, strong stretching flow components are introduced. When typical values for η_d, η_m, σ and $\dot{\gamma}_m$ in shear flow are introduced, R^c is calculated to be 0.2 mm. Thus many small bubbles are probably created. The existence of large number of small bubbles in the melt would significantly increase the total area for diffusion to occur, thus significantly enhancing mass transfer in the gas injection section of the extruder.

It is worth noting that, since the C_a^c vs. η_d/η_m for stretching flows is lower and viscosity-ratio-independent, kneading elements would break up gas bubbles into smaller diameters than 0.2 mm, increasing mass transfer rate.

It is reasonable to believe that foaming in the gas injection/dissolution region is influenced by the operating conditions such as screw speed, polymer throughput and gas injection pressure.

Gas dissolution in the gas injection zone is enhanced due to foaming, and the limit of gas dissolution is the amount that could be dissolved if equilibrium is achieved. This limit is calculated based on Henry's law and plotted in Figures 5.2 through 5.5. As shown in Figure 5.2, for CO_2, the actual total amount of gas in polymer melt is less than that calculated from Henry's law, the solubility limit; for Argon, the actual total gas weight

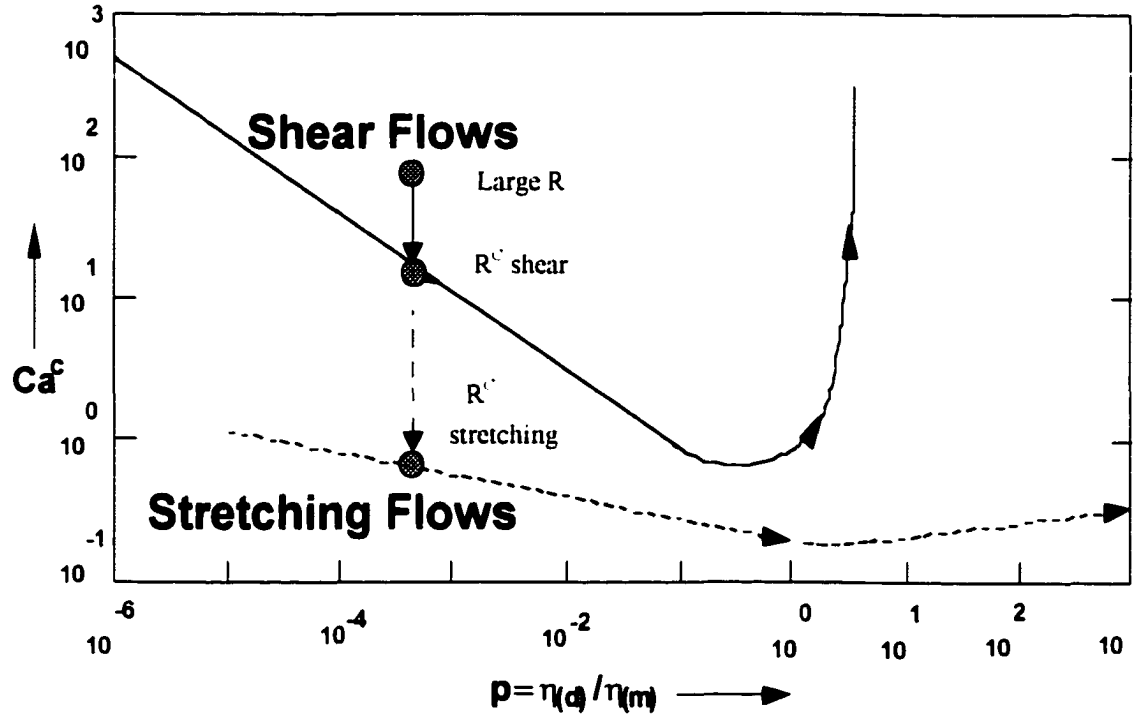

Figure 5.6 Laminar Dispersive Mixing for Dilute Newtonian Systems (Grace, 1982)

fraction is about the same as the solubility limit; for N_2, the amount of gas in the melt actually exceeded the solubility limit. Given the short residence time and the low diffusivity values of these gases, it is very less likely that the diffusion process could reach equilibrium in the short gas injection section of the screw. This indicates that gases are carried down stream in form of foam through the compression zone and into the metering zone. Unlike the gas dissolution process, which is dictated by solubility, diffusivity, mass transfer area and residence time, the "carry over" or entrainment is likely to be a volumetric process, so it is reasonable to assume that under similar conditions, the amount of "carry over" is similar for the three different gases. While the contribution of this amount of gas is not significant enough to exceed the solubility limit for carbon dioxide, it is enough to surpass the solubility limit of nitrogen under the gas injection pressure due to the much lower solubility of the nitrogen gas. Significant amount of gas was "carried" trough the compression-zone into the melt as it foams and got dissolved in the melt under much higher pressure during compression and in the metering zone, this is also facilitated by enhanced mixing/homogenization and longer residence time. Air entrainment in the compression zone in extruders has been observed and documented (Tadmor and Gogos, 1979). But this phenomenon here is much more pronounced due to foaming. From a gas dissolution point of view, foaming in the gas injection/dissolution zone is desirable because it facilitates mass transfer and helps to "place" more gas in solution, this is especially helpful when inert gases such as N_2 with very low solubility in the polymer melt are used as blowing agents. But, compression and pumping of the compressible foam formed in this region could make the extrusion process to surge and possibly is one of the main factors contributing to process instability, which is one of the main problems for a suitable foam

extrusion process. In industrial foaming processes, narrow operating window and accurate process control requirements often necessitate the use of a melt pump after the screw for satisfactory pressure control.

The effects of screw speed and the polymer throughput on gas dissolution characteristics were simulated using the model. The results are presented in Figures 5.6 and 5.7. These results show that, based on the mass transfer mechanisms described in the model, the amount of gas dissolved in the melt increases with increasing screw rpm under fixed polymer feed rate and gas injection pressure and decreases with increasing polymer throughput under fixed screw rpm and gas injection pressure. The main factors affecting gas diffusion are mass transfer areas as shown in the model, residence time and the free surface renewal rate. Higher screw speed gives higher free surface renewal rate and larger barrel film surface area, both of which contribute to increased rate of gas dissolution. At a fixed screw speed, if an increase in polymer throughput takes place, when starved, residence time stays constant, but, the degree of fill is increased and the barrel film surface area is decreased. These contribute to a decreased gas dissolution rate.

The foaming effect is not considered for these simulation results. Screw speed and polymer throughput could have profound effects on the gas dissolution rate as discussed earlier. For example, an increased screw speed could, on one hand, enhance foaming by providing enhanced whipping and frothing, and on the other hand, reduce the degree of foaming by completely breaking some of the bubbles in the foam. It is considered to study the effects of these processing on the gas dissolution characteristics experimentally. Unfortunately, experiments for studying these effects were not successful. The process

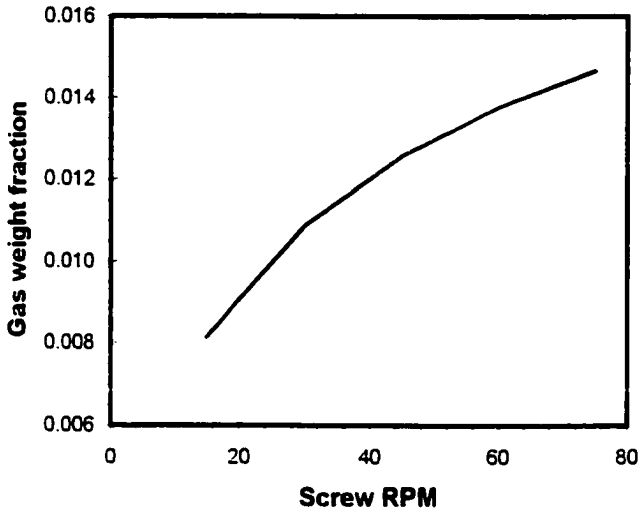

Figure 5.7 Effect of Screw Speed on Gas Dissolution Calculated from the Model (CO_2 in PS, Polymer Throughput: 1300g/h; Gas Injection Pressure 3770 kPa)

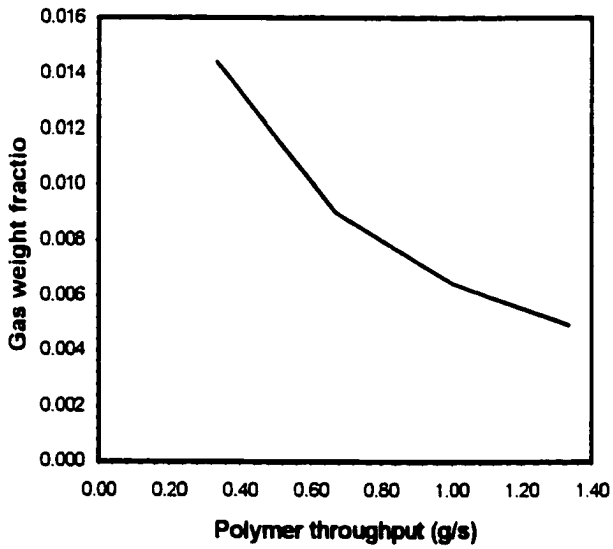

Figure 5.8 Effects of Polymer Throughput on Gas Dissolution Calculated from the Model (CO_2 in PS at 215°C, Screw rpm: 60; Gas Injection Pressure 3770 kPa)

requires a rather narrow window of operating conditions in terms of polymer feed rate and screw rpm combinations. For starved feeding operation, under a fixed rpm, a proper seal can not be formed to prevent gas leaking backward due to the low degree of fill. Similarly, the screw speed can not be varied in a large range when the polymer feed rate is fixed. The effects of processing conditions on the gas dissolution characteristics were further studied using a twin-screw extruder and the results are given in detail in the next chapter.

CHAPTER 6

EFFECTS OF PROCESSING CONDITIONS

In industrial practice, both single screw and twin-screw extruders are used to make foamed products. Twin-screw extruders generally have much better mixing characteristics, hence provide better thermal and material homogeneity of the gas-laden melt, which contributes to making good quality foamed products. The in-line window system developed in this study was connected to a twin-screw extruder to first test the machine independence of the method, and then study the effects of processing conditions on the gas-polymer solubility and gas dissolution characteristics in the extruder. The versatile nature of the twin-screw extruder operation allows varying processing conditions in a wide range, thus making it possible to accomplish these tasks.

6.1 Equipment and the Polymer-Gas System

The extruder used for this part of the study is a 34mm intermeshing, co-rotating twin-screw extruder (Leistritz LSM34) having a L/D of 36. All other equipment and the data acquisition system were the same as in the single screw case.

For easy operation and comparison purposes, all the experiments were conducted only for the polystyrene–carbon dioxide system.

CO_2 gas was injected in the middle of the barrel in the same way as in the single-screw extruder from a gas cylinder. The gas flow rate was metered and digitized into a computer for on-screen monitoring and off-line analysis. The important parameters such as

gas injection pressure, die temperature and pressure and window temperature and pressure were also digitized into the computer.

The screws were specially configured to serve the purposes of appropriate melting, effective melt seal, adequate compression and good mixing. A schematic of the screw configuration is given in Figure 6.1.

6.2 Testing of the In-Line Solubility Measurement System

A series of preliminary solubility measurement experiments conducted to test the window system with the twin-screw extruder indicated that he system worked very well.

One of the major problems encountered during the single-screw experiments was that when the window pressure was adjusted, the pressure change propagated toward the back of the extruder and affected the gas flow rate significantly, requiring long periods of time to stabilize the process after each adjustment, and possibly causing errors. During the twin-screw extrusion experiments, this was substantially reduced.

A comparison of solubility data measured using the twin-screw extruder–window system with that obtained earlier in the single-screw experiments is presented in Figure 6.2. The twin-screw extrusion results were obtained at a polymer feed rate of 2.4 kg/hr in comparison to the feed rate of 1.32 kg/hr used in the single screw experiments. The 30 rpm screw speed used in the twin-screw experiments is higher than that used in the single-screw experiments (15 rpm). The results show very good agreement between those data obtained from two different systems. More importantly, the regression curve for the new data passes through zero. The linear regression curve for the twin-screw data gives a solubility value of 0.0028 $cm^3[STP]/g \cdot kPa$ with $R^2=0.9842$, while for the results obtained

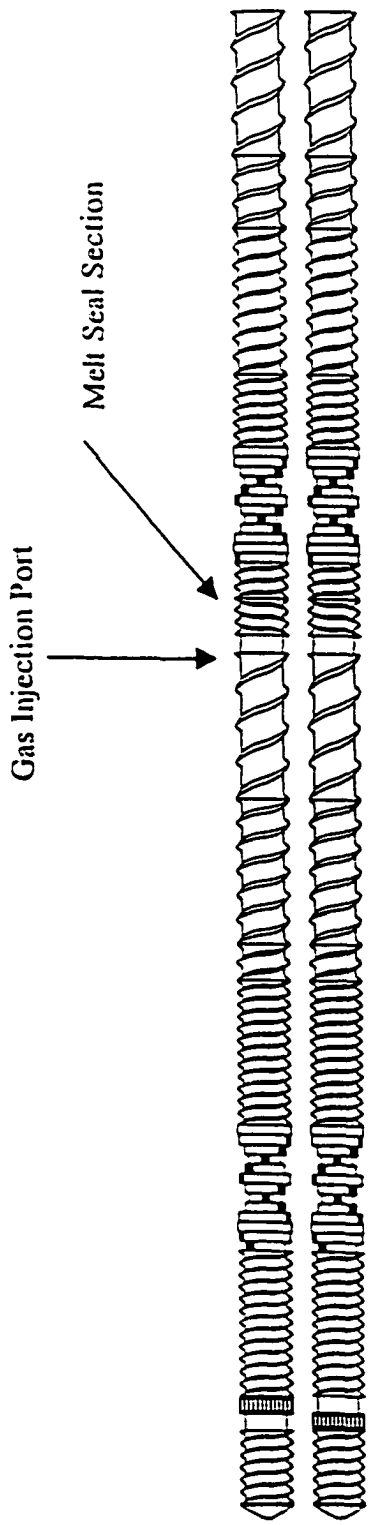

Figure 6.1 Schematic of the Screw Configuration for the Twin-Screw Extruder

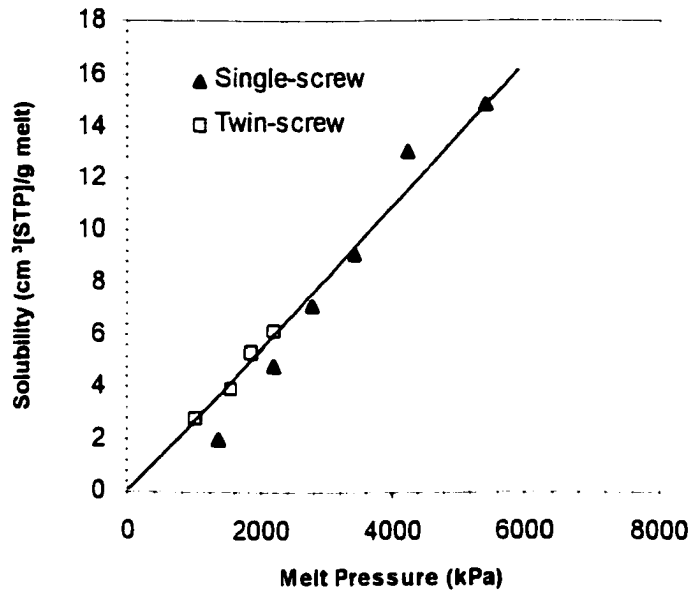

Figure 6.2 Comparison of Solubility Data Obtained from Single Screw and Twin-Screw Experiments (CO_2 in PS at 215°C) – Line Represents Regression of TSE Data Only

from the single extruder experiments, as mentioned earlier, a solubility value of 0.0027 cm^3[STP]/g•kPa with R^2=0.9459 was obtained. This further confirms that inadequate homogeneity of the gas-laden melt in the single-screw case was responsible for the poor consistency of solubility data of the systems studied under low pressures.

In the twin-screw extruder, the screws were configured with kneading blocks after the gas injection section for improved mixing. As shown in Figure 5.6, the stretching flow in this region is far more effective in breaking the gas bubbles into many more bubbles with much smaller diameters than in a single screw extruder where shear flow dominates. This would contribute significantly to enhanced rate of gas dissolution and possibly to improved homogeneity of the gas-laden melt.

Due to the limitations on the flow meter range (500 cm^3[STP] /min maximum), the pressure range studied here is not as large as that in the single screw case.

This part of the study has confirmed that the in-line method developed here satisfies one of the basic requirements of a valid methodology – machine independence. Good mixing has been shown to be an important requirement for good data consistency.

6.3 Effects of Processing Conditions on the Gas Solubility in Polymer Melts

Two main processing conditions, screw speed (rpm) and polymer throughput were varied to study the effects of these parameters on the solubility characteristics.

Figure 6.3 shows the screw rpm effects where screw speed was varied while keeping the polymer feed rate constant. These results show that solubility is independent of extruder screw rpm; this is true at least for the screw speed range studied. During this set of experiments it was observed that when the screw speed is high, more heat is

generated in the extruder, and the thermal homogeneity of the gas-laden melt becomes poorer than when screw speed is low.

The effects of polymer throughput are given in Figure 6.4 where polymer feed rate was varied while screw speed was kept constant. These results show the correlation of solubility with polymer throughput. Solubility seems to decrease with increasing polymer throughput. It should be noted that when the polymer throughput is high, the linear velocity of the melt passing the window area is high, so the data obtained are possibly less accurate. Also, at the low screw speed (30 rpm) used in this set of experiments, when polymer feed rate is high, the degree of fill is high and the residence time is reduced; as a result, the mixing in the extruder is relatively poor, which gives poor thermal and material homogeneity. Results from the single extrusion experiments have shown that this will result in underestimated solubility data. Even after considering all these factors, correlation between solubility and polymer throughput appears to exist.

Increasing polymer throughput would directly increase the shear rate on the wall at the window where bubble nucleation occurs. Lee (1993) studied shear effects on thermoplastic foam extrusion using a cavity model as shown in Figure 6.5. In a foaming process, it is a virtually heterogeneous nucleation in nature, at least thousands of nucleators clump together to form a nucleating site (Lee, 1993). In cases where no nucleating agents are used, the inherent micro-crevices of the melt are considered as potential nucleating sites (Biesenberger and Lee, 1986). It can be envisioned that the clump has a porous surface, which is typified by Figure 6.5a, where R is the radius of the curvature, and θ is the wetting angle. It will not be totally wetted by the molten polymer.

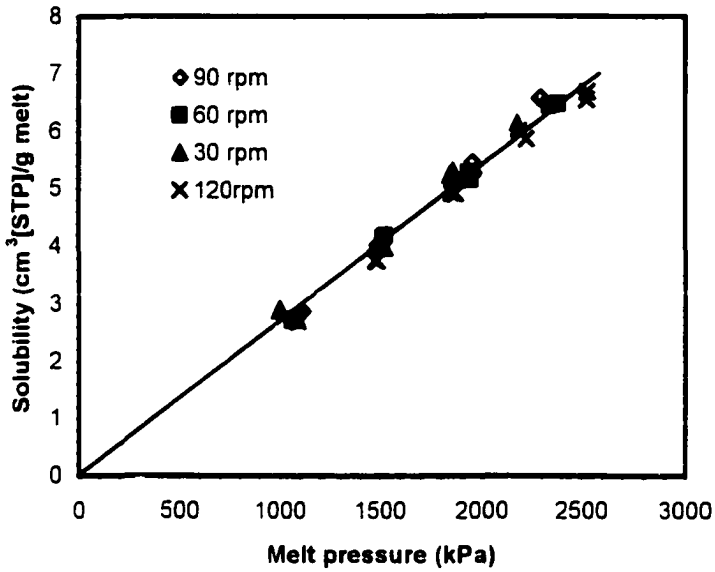

Figure 6.3 Effect of Screw Speed on the Solubility of CO_2 in PS at 215°C (Constant Polymer Throughput at 3.76 kg/h)

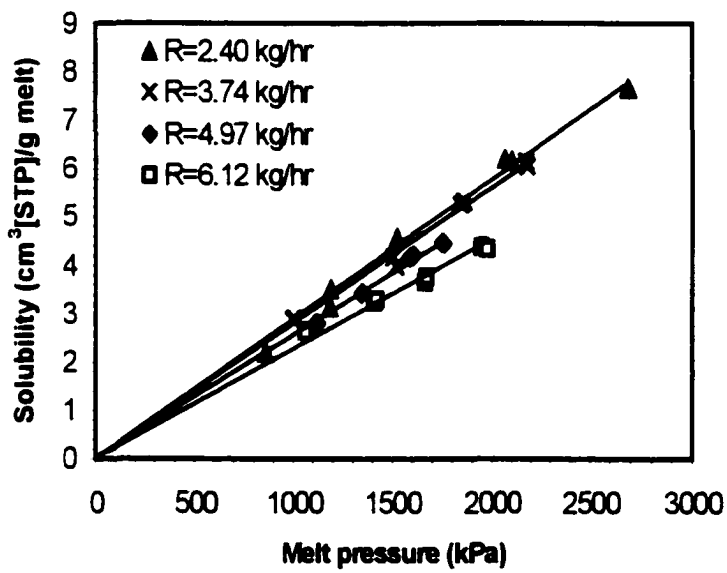

Figure 6.4 Effect of Polymer throughput on the Solubility of CO_2 in PS at 215°C (Constant Screw Speed at 30 rpm)

As blowing agent is introduced into the molten polymer, it tends to diffuse into the gas phase cavity end to establish equilibrium if adequate mixing and/or long enough residence time can be achieved, as shown in Figure 6.5a. As the surrounding pressure decreases, the gas phase in the conical end will increase its volume and tend to maintain proper radius of curvature, R_{cr}, which is governed by:

$$R_{cr} = \frac{2\sigma}{\Delta P} \tag{6.1}$$

where ΔP is the pressure difference between ambient pressure and gas vapor pressure and σ denotes surface tension. It is conceivable that the meniscus changes from an initial negative radius to a positive one as the ambient pressure drops to less than the vapor pressure, as indicated in Figure 6.5b. The contact angle decreases as ΔP decreases and reaches to a yield point when the gas phase slips to the cavity mouth as illustrated in Figure 6.5c. As the surrounding pressure keeps decreasing, the gas phase will grow until it overcomes the confining critical surface tension resistance; this situation is shown in Figure 6.5d. It will grow until detaching from the cavity to foam an unstable gas bubble as shown in Figure 6.5e. The presence of high shear can certainly help "pull" the gas phase out of the solid cavity, hence assisting nucleation. Through a force balance approach (based on the situation shown in Figure 6.5 d), Lee (1993) obtained the factor that dictates bubble nucleation, the familiar Capillary number, C_a, defined as:

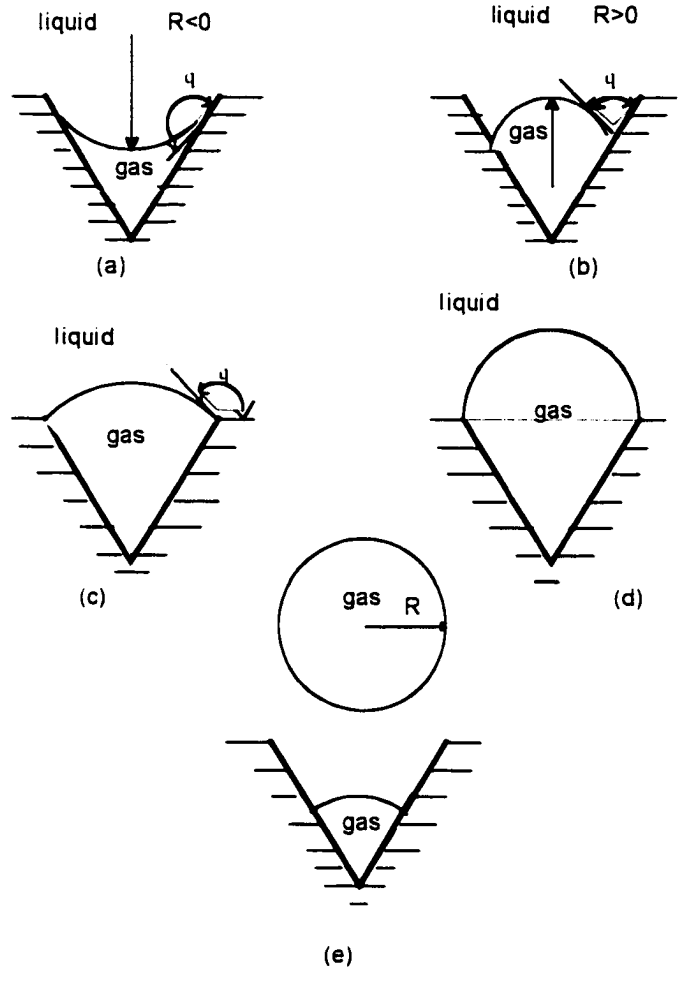

Figure 6.5 Illustration of the Cavity Model (Lee, 1993)

$$C_a = \frac{R\eta\bar{\dot{\gamma}}}{4\sigma} \tag{6.2}$$

where R is the cavity mouth radius, η is viscosity, and $\bar{\dot{\gamma}}$ is average shear rate. Lee's experimental results confirmed that the number density (# of cells/cm^3) of the foamed product is proportional to the Capillary number for the system he studied. He found that this was true for the nucleating agent (talc) levels tested and also for the same system without nucleating agent.

Recent research work at the National Research Council of Canada (NRC) has shown that introduction of shear lowers solubility (Caron et. al., 1997). They measured solubility of three different blowing agents, isopropanol, HCFC 142b and HFC 134a in polystyrene in a pressure vessel and varied the mixing rpm from zero to 120, 60 and 180 for the three systems respectively. Solubility reduction of 4.5%, 11.7% and 13.4% was obtained for the three systems studied.

6.4 Effect of Nucleating Agents on the Gas Solubility in Polymer Melts

In thermoplastic foam extrusion, the presence of a nucleating agent is, in most cases, necessary to control cell size and cell distribution. Hansen and Martin (1964; 1965) have reported that well-dispersed particulate materials (e.g., metal particles, sodium aluminum silicate, SiO_2, Fe_2O_3) act as nucleating sites for the formation of bubbles from the dissolved gas and help to create a uniform cell structure in the extruded foam. In the

presence of nucleating agents, bubble formation would occur at lower gas concentrations than in the absence of nucleating agents (Han, 1981). In other words, heterogeneous nucleation, providing a great abundance of nucleating sites within the supersaturated melt, is much more effective than homogeneous nucleation in facilitating bubble formation and producing uniform cell structure (Han, 1981). Hansen and Martin (1965) reported that a tenfold increase in nucleator particle concentration caused a thousandfold increase in the number of bubbles, and a fiftyfold decrease in the volume of each bubble, at approximately the same level of supersaturation.

Research has shown that increasing shear rate promotes nucleation; this effect increases as nucleating agent level increases (Lee, 1993). It is a long asked question as to how does the nucleating agent level affect the solubility characteristics. In this study, a series of experiments were designed to study this effect. An experimental grade, fine talc with median particle size of 1.6 micron and a top cut of 10 micron (Benwood 2002 manufactured by ZEMEX Industrial Minerals) was used as the nucleating agent. Solubility measurements were conducted at two different levels of talc concentrations, 0.1% and 0.3 % by weight. It should be noted that the used levels are much higher than those normally used in industrial extrusion foaming processes. The results and their comparison with data obtained without talc are presented in Figure 6.6. It is shown that talc concentration does not affect CO_2 solubility in polystyrene. A very interesting observation is that the data are more scattered than those obtained in the absence of nucleating agents. Experiments on extrusion foaming of the same material using CO_2 as blowing agent (Zhang, 1997) has shown that in the absence of nucleating agent, the resulting foam is comprised of a small number of very large cells. And, when nucleating agent (0.05% talc) was used, the foam

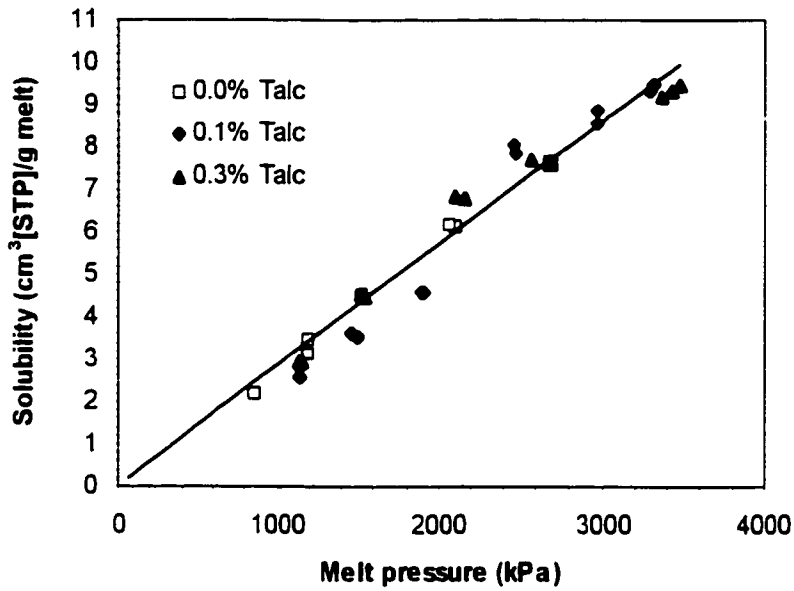

Figure 6.6 Effect of Talc Concentration on Solubility of CO_2 in PS at 215 °C (Screw Speed: 30 rpm; Polymer Throughput: 2.40 kg/h)

cell size was reduced significantly (at least by a few hundredfolds) with increased cell density. This indicates that when nucleating agent is present in the supersaturated melt, bubble nucleation is more instantaneous and, possibly more explosive, in which case bubble nucleation happens at a higher degree and a larger scale. This might have contributed to the scattering of the experimental data.

It is generally recognized that nucleating agents are critical in foaming amorphous polymers. For semicrystalline polymers, however, some crystals may form under foaming temperatures without any other agents, and these crystals could serve as sites for bubble nucleation.

6.5 Gas Dissolution in Twin-Screw Extruder during Foam Extrusion

In Chapter 5, it has been shown that gas dissolution in the gas injection area in the single-screw extruder only accounts for a portion of the gas which is actually in solution as measured downstream. Significant amount of "carry over" exists which may contribute to process instability. It is beneficial to know the gas dissolution mechanisms in the twin-screw extruder and their relation with major processing conditions such as screw speed and the polymer throughput. This information is very useful for design and process control purposes.

The actual amount of CO_2 gas in polymer (PS) solution was measured downstream at the window using the window system and compared with the values calculated from Henry's law based on the corresponding gas injection pressure. Figure 6.7 shows the comparison for different gas injection pressures under the same screw speed and polymer throughput. These results clearly show that in the twin-screw extruder, the

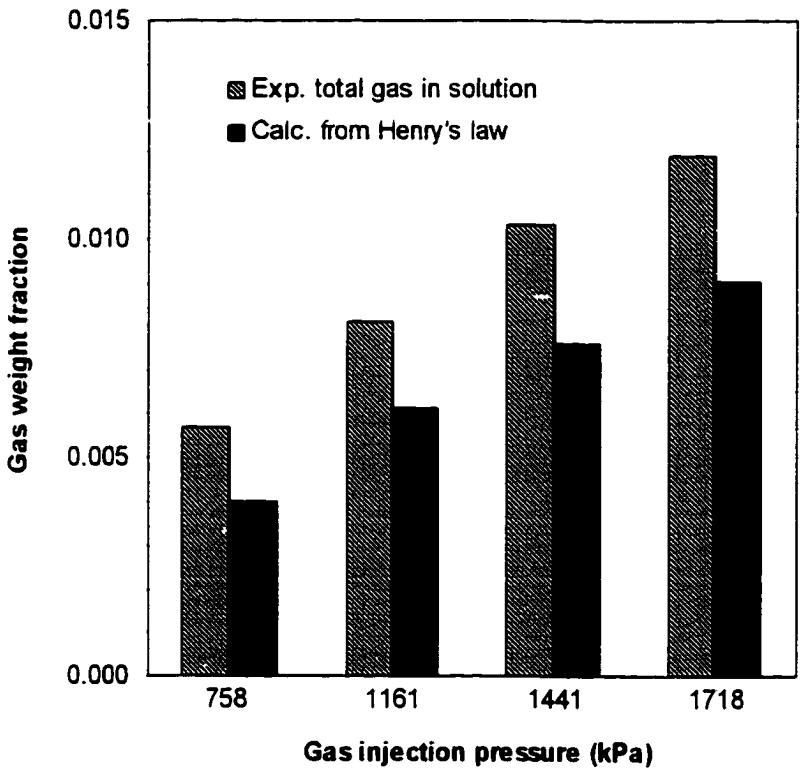

Figure 6.7 Comparison of CO_2 Gas dissolution with the Solubility Limit
(Screw Speed 30 rpm, PS Throughput 3.76 kg/h, Melt Temperature at Window 215 °C)

actual amount of gas dissolved in the system surpassed the equilibrium limit corresponding to the gas injection pressures, which again indicates the existence of significant "carryover".

The effect is much stronger in the twin-screw extruder than in the single screw extruder. This is likely related to the difference on the manner of the operation and the screw configuration between the two different types of extruders. The effects of polymer throughput and screw speed on the gas dissolution are shown in Figures 6.8 and 6.9 respectively. The actual amount of gas in polymer solution as measured downstream at the window area was plotted versus gas injection pressure in both cases.

Figures 6.8 indicates that the gas weight fraction in the melt decreases with increasing polymer throughput. This is reasonable because an increase in throughput will increase the degree of fill thus reducing the mass transfer areas. Also, the residence time is reduced, so the gas dissolution through diffusion is reduced.

Figure 6.9 shows that gas weight fraction in the melt does not change with screw speed. This is somewhat surprising because as discussed in 5.2, increasing screw speed would enhance mass transfer through diffusion. If this is true, the results shown in Figure 6.9 really mean that the degree of "carryover" decreases with increasing screw speed. This may be an indication that the "carryover" happens mainly through a "frothing" type of mechanism, since high screw rotation would likely break the froth in the compression zone, thus reducing the degree of entrainment.

6.6 Summary

The in-line window system was connected to a co-rotating (Leistritz) twin-screw extruder to measure solubility of CO_2 in PS melt, the results were compared with those obtained from the single screw extruder experiments for the same system under similar conditions. Results obtained with the twin-screw extruder configured for improved mixing indicate better data consistency, presumably as a result of enhanced homogenization and dissolution.

The effects of the main processing conditions such as screw speed and polymer throughput on the gas solubility and gas dissolution characteristics were studied using the in-line window - twin-screw extruder system for the system polystyrene-carbon dioxide. It was found that screw speed does not affect the gas solubility for the range studied. It was also found that gas solubility decreases with increasing polymer throughput, indicating that increasing shear lowers gas solubility. This finding is consistent with literature results obtained using a high-pressure vessel for different polymer-gas systems (Caron, et al., 1997).

Much more significant "carryover" exists during the twin-screw extrusion foaming compared with the case of a single-screw foam extrusion. It was found that the gas weight fraction in the melt, as measured downstream at the window, decreases with increasing polymer throughput while it remains unchanged with changing screw speed.

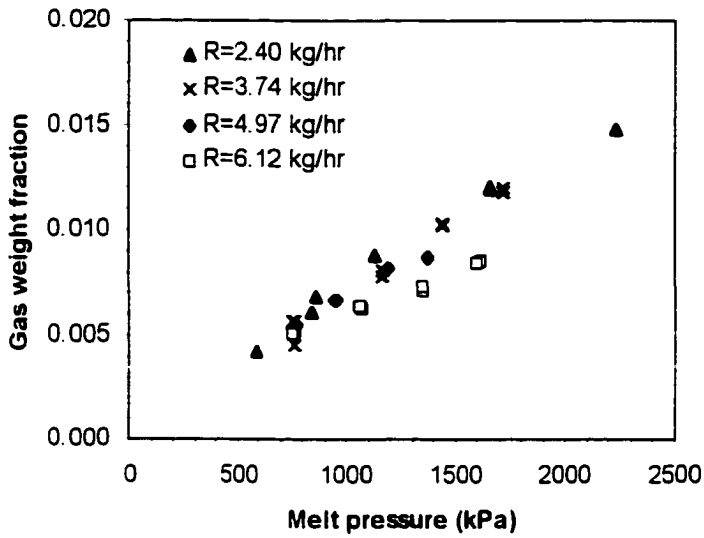

Figure 6.8 Effect of Polymer (PS) Throughput on the CO_2 Gas Dissolution Characteristics (Screw Speed 30 rpm, Melt Temperature at Window 215°C)

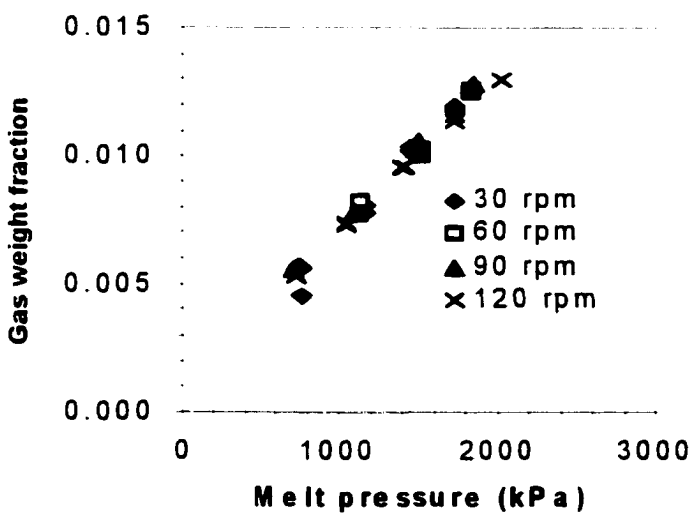

Figure 6.9 Effect of Screw Speed on the CO_2 Gas Dissolution Characteristics (Polymer Feed Rate 3.76 kg/h, Melt Temperature at Window215°C)

CHAPTER 7

APPLICATION OF SOLUBILITY DATA ON EXTRUSION FOAMING OF POLYETHYLENE TEREPHTHALATE

Extrusion foaming of polyesters, especially semicrystalline resins such as PET, is a relatively new and increasingly active area presenting several challenges. Most PET resins have rheological properties at processing temperatures (>250°C) that are not conducive to foaming. The low melt viscosity and low melt strength and " melt elasticity" of the polymer do not contribute to controlled cell expansion and stabilization of the growing bubbles (Throne, 1996; Boone, 1996). Hydrolytic degradation due to water given-off as a decomposition by-product of certain CBAs can further reduce foamability. PET resins with improved rheology and melt strength can be produced during esterification or by post-reactor processing, as, for example, by reactive extrusion. Modification in the melt is carried out through chain extension /branching reactions, primarily between the carboxyl/hydroxyl end groups and di- or polyfunctional reagents containing oxazoline, isocyanate, epoxy, carbodiimide, anhydride, hydroxyl, tertiary phosphite, phthalimide and other groups (Brown, 1992). Production of high IV (>1.1 dl/g) and high melt strength foamable PET by extruder mixing, followed by solid state reactions has been recently described (Al-Ghatta, et al., 1996; 1997).

In this part of the study, a commercial PET resin, the same material as used for solubility studies in Chapter 4, was foamed in a single screw extruder using inert gases (CO_2, N_2 and Ar) as blowing agents. This was part of a larger effort to develop extrusion technologies to foam PET using inert gases as alternatives to traditional PBAs such as

HCFCs and VOCs. The emphasis here is to analyze the foaming process using the information obtained in this study including the solubility of the three gases in PET and their dissolution characteristics in the extruder during the foaming process.

7.1 Experimental Procedures

As shown in Figure 7.1, a 32 mm diameter, 40 L/D Killion segmented single screw extruder (the same extruder and screw configuration as used in solubility studies) equipped with a 250 mm wide sheet die and a three stack chilled roll assembly was used for this part of study. Carbon dioxide, nitrogen and argon gases were used as blowing agents with no additional nucleating agents. The resin used is a commercially available CPET (Shell Traytuff 9506) with a nominal IV of 0.95.

A number of foaming experiments were conducted for each gas blowing agent to cover a wide range of gas injection pressures ranging from 1380 kPa (200 psi) to 5500 kPa (800 psi). During each experiment, the barrel and die temperatures were adjusted to the levels that are optimal for making the best quality foam product. The gas flow rate was monitored using the mass flow mater as described in the solubility measurement procedures, and also recorded for off-line analysis. The product was collected and analyzed in terms of foam density and cell structure.

The polymer pellets were dried in a vacuum oven at 120°C for about 20 hours prior to each experiment. The runs were carried out at a screw speed of 20 rpm with a polymer throughput of 2.38 kg/h.

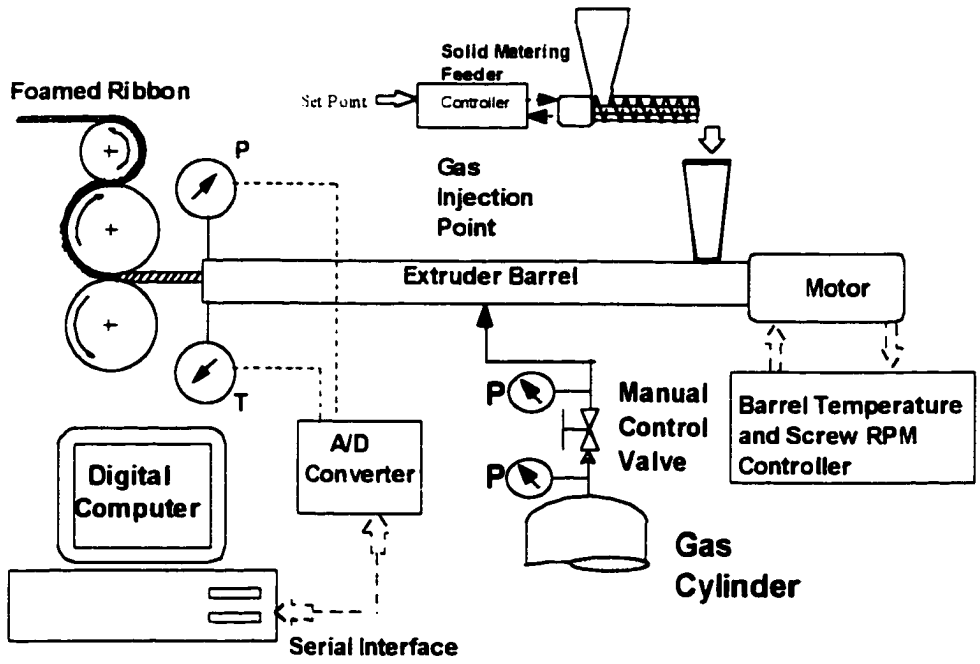

Figure 7.1 Schematic of the Experimental Setup for Extrusion Foaming of PET

7.2 Results and Analysis

A summary of the experimental conditions is given in Table 7.1. The actual foaming temperature (measured directly for the melt at the die) was kept very close to the melting point of the material, and the variation from run to run was relatively small.

The average gas flow rate as function of gas injection pressure is plotted in Figure 7.2. It is shown that the gas flow rate is proportional to the injection pressure for the three gases in the same order of their solubility in PET, i.e., CO_2>Ar>N_2 as shown in section 4.2.

As mentioned earlier, in all the foaming runs, the melt temperature was adjusted to be very close to the crystallization temperature of the gas-laden melt under the specific conditions. So the variations in the lowest melt temperature achievable under different gas flow rates are indications of reduction of viscosity of the gas-laden melt and also depression of the melting temperatures of the polyester material. Figure 7.3 presents the actual melt temperature during foaming as a function of gas flow rate for the three different blowing agents. These results show that for CO_2, the melt temperature decreases with increasing gas flow rate in the studied range. Decreasing trends appear also to be followed by Ar and N_2 in their respective gas flow rate ranges. Due to the differences in their solubility, the amount of gas dissolved into the melt system varies in the order CO_2>Ar>N_2, and the actual minimum foaming temperature achieved is in the order N_2>Ar>CO_2. Overall, regardless of the type of gas, the melt temperature reduction, assumed to be equivalent to depression of crystallization temperature, is roughly proportional to the amount of gas dissolved in the melt. Considering the amount of gas dissolved, this reduction is very limited. For example, for the PET-CO_2 system, at the

Table 7.1 Summary of Experimental Conditions for PET Foaming with CO_2, N_2 and Ar

Gas	Melt Temperature (°C)	Injection Pressure (kPa)	Die Pressure (kPa)	Average Flow Rate (cm^3STP/min)
Ar	262.8	1380	3240	30.3
Ar	261.0	2760	5030	69.8
Ar	260.0	4160	5375	130.0
Ar	260.0	5510	7225	157.0
N_2	265.0	2090	5445	17.8
N_2	262.0	2760	6425	13.9
N_2	261.5	4210	7250	25.6
N_2	261.6	5540	7940	80.8
CO_2	260.2	1430	8550	66.7
CO_2	259.0	3050	7470	219.0
CO_2	259.0	4040	5735	301.7
CO_2	258.4	5340	9200	394.0

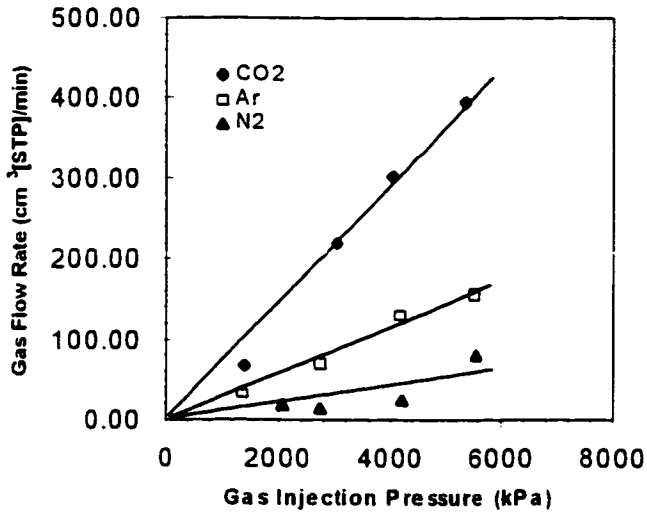

Figure 7.2 Gas Flow Rate during Extrusion Foaming vs. Gas Injection Pressure

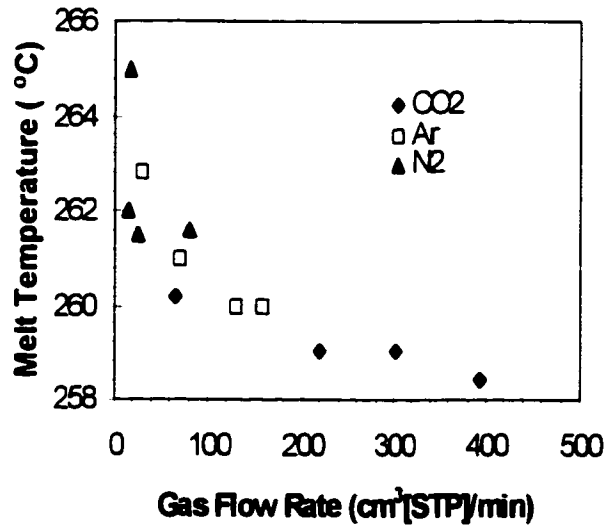

Figure 7.3 Melt Temperature during Foaming vs. Gas Flow Rate

highest gas flow rate (corresponding to 5340 kPa gas injection pressure), only a 4-5 °C temperature reduction was achieved.

Zhang and Handa (1997) studied CO_2-assisted melting of semicrystalline polymers using a DSC equipped with high-pressure vessels rated to 100 atm. Their results show that while CO2 is effective in depression of the crystallization temperature of melt-crystallized syndiotactic polystyrene (sPS), this effect on PET is very limited. Calculations based on their results show that under the same pressure as used here (i.e., 5340 kPa), 11°C of reduction of the crystallization temperature was obtained for the melt-crystallized sPS, while the melting temperature reduction for PET is only about 4°C. Compressed N_2 under similar conditions was found to have no effect on the melting behavior of PET. The authors attributed this phenomenon to the very low solubility of the N_2 in the PET material.

This "ineffectiveness" in crystallization temperature depression presents a further challenge to PET foaming, since the high temperature does not favor better foaming efficiency.

Foam density as a function of gas injection pressure is presented in Figure 7.4. It has been shown earlier that gas flow rate is proportional to gas injection pressure. One would expect that foam density would show a similar trend. Interestingly, as shown in Figure 7.4, the differences between different gases are relatively small. Initially, the foam density decreases as the amount of gas in the polymer melt increases (as injection pressure increases). At around 2500 kPa gas pressure, the curve levels off, and further introduction of the blowing agent does not result in further reduction in foam density. This suggests

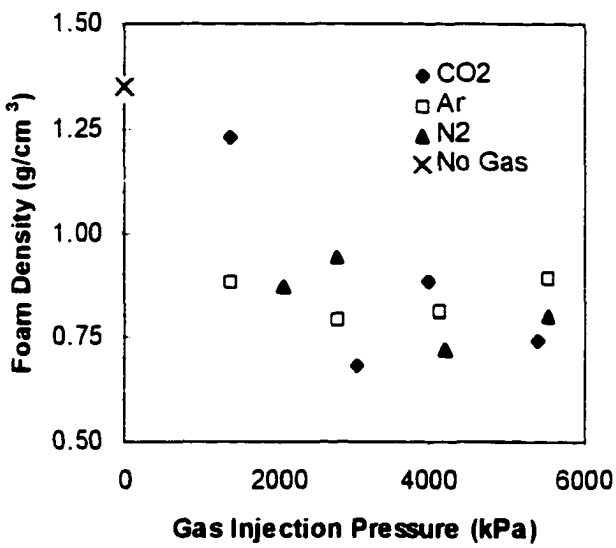

Figure 7.4 Foam Density as a Function of Gas Injection Pressure

that significant gas loss happened when the amount of gas injected into the system was higher than a certain value.

In a continuous foaming process, the nucleated cell is of a highly unstable nature, and, it tends to grow with a rate depending upon system parameters such as degree of supersaturation, number of bubbles per unit volume, solubility of gas in the polymer matrix, polymer viscosity, diffusion coefficient, and surface tension forces. Cell wall thickness decreases as density gets lower. Due to this phenomenon, the cells become weak and prone to rupture (Lee and Ramesh, 1996). A numerical study by Lee and Ramesh (1996) showed that gas loss mainly happens during the later stage of growth. The authors argued that the initial growth is mainly pressure gradient controlled, and the gas escape effects become important when the role of diffusion dominates. The blowing agent escape from the surface due to a shorter diffusion path to the surface than to the bubble is dictated by the ratio of external surface area to internal surface area.

The gas loss in this study is very significant. Gas is lost mainly through cell collapse and/or skin rupture due to low melt strength of the material under processing conditions. The effect is further amplified by the use of a flat sheet die where the foam sheet has a very large surface area to volume ratio.

To characterize gas loss, blowing agent efficiency, E_{BA}, defined as the ratio of the theoretical amount of BA required (assuming all gas is utilized for foaming the material) to make the foam, to the actual amount of gas used, is calculated and plotted in Figure 7.5. These results show that as gas injection pressure increases, the blowing agent efficiency decreases, indicating significant gas loss during the foaming process. The efficiency of Ar

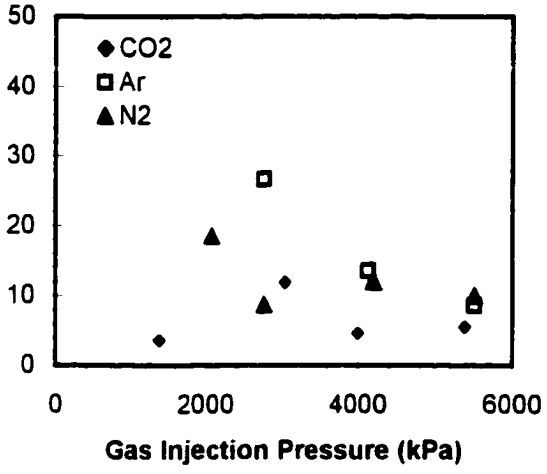

Figure 7.5 Blowing Agent Efficiency vs. Gas Injection Pressure

and N_2 was much higher than that of CO_2, but when pressure reaches a certain point, gas loss becomes significant, and BA efficiency for all gases drops rapidly. This dictates that rheological modification of the polyester material to higher melt strength/elasticity is necessary for this process to be efficient.

7.3 Summary

A commercial PET was foamed in a segmented single screw extruder equipped with a 250 mm wide flat sheet die using inert gases (CO_2, Ar and N_2) as blowing agents. Foam density was found to be a decreasing function of increasing gas injection pressure, but with a plateau apparently reached at relatively low gas pressure. Further increase of the gas pressure did not result in reduced foam density, mainly due to gas loss during foam growth, possibly through cell collapse and/or skin rupture.

Gas flow rate was found to be proportional to injection pressure for the three gases used in the same order of their solubility in the polymer. Crystallization temperature depression as indicated by the melt temperature values at the die was shown to depend on the solubility of the respective gases. The type of gas was found insignificant in affecting foam density when the gas injection pressure is high, again, due to low blowing agent efficiency.

Blowing agent efficiency, along with other criteria, such as foam quality and density, can be used as an important tool to characterize the feasibility of a foaming process.

CHAPTER 8

SUMMARY AND CONCLUSIONS

A novel in-line method for measuring gas solubility in thermoplastic melts in extrusion foaming equipment has been developed in this study. This method utilizes video microscopy with a foaming extruder to generate solubility data by observing the onset of gas bubble nucleation/dissolution.

Compared with the traditional off-line methods, this continuous in-line method has a number of advantages. First, the in-line method measures solubility in a foaming process, which does not need delicate equipment such as a microbalance, and deals with much greater amount of material hence giving better accuracy. Also, this method does not need the time-consuming calibration process as required by most of the other methods, thus avoiding possible errors originating from those processes.

Secondly, this method can be easily used to obtain solubility data at high pressure and temperature near actual foaming conditions. These data could be used directly to characterize and control a foaming process and also provide guidelines for blowing agent selection, foam process design and optimization.

Thirdly, since the residence time of the polymer in the extruder is short (typically 5-10 minutes), this in-line method may allow solubility determination for temperature sensitive polymers that would otherwise degrade in other measurement methods.

Finally, the system can be used to study the dynamics of the bubble formation and dissolution in a foaming process. Also, the unique nature of the methodology allows studying the effects of processing conditions on the gas solubility characteristics, which is

not accomplishable by the traditional off-line methods where only thermodynamic data could be obtained. If used with a reactive extruder, this system is potentially very useful for studying the effects of polymer modification on gas solubility characteristics.

Data obtained for the PS-CO_2 system compared favorably with literature equilibrium data obtained using off-line methods. Solubility data of CO_2, Ar and N_2 in molten PET were obtained. For this system, such data have not been available in the literature prior to this work. Temperature dependence of solubility of different gases in PS and PET were studied in a small temperature range. The results showed similar trends with literature data for both PS and PET systems.

Solubility data of CO_2 in polystyrene were also obtained using a twin-screw extruder. Significant improvement in data consistency was observed for the twin-screw experimental data; this indicates the importance of enhanced mixing in affecting the solubility values obtained from the in-line method.

The effects of principal processing conditions and the level of nucleating agents on the solubility characteristics were also studied. The results show that the measured CO_2 take-up values in polystyrene melt are affected by polymer throughput, suggesting that an "apparent solubility" is measured. The addition of nucleating agent (talc) into the gas-laden melt does not affect the gas solubility within the practical range of concentrations.

Gas dissolution mechanisms were studied through mathematical modeling using a simple penetration mass transfer model over the gas injection section. Comparison of model predictions with experimental results and the solubility limit revealed that the model is insufficient in explaining the very complex phenomena occurring inside the extruder. This suggests the existence of other mechanisms that contribute to gas dissolution over the

entire extruder length. The results indicated that certain amount of gas could be entrained into the system through the compression zone of the extruder during the foaming process, causing the actual amount of gas dissolved in the melt to surpass the solubility limit corresponding to the gas injection pressure.

Extrusion foaming of PET in a flat sheet die was performed in a single screw extruder using inert atmospheric gases (CO_2, Ar and N_2) as blowing agents. Analysis of the foaming process showed that the foaming operation could only be done at relatively high temperatures (close to the crystallization temperature of the PET material) due to the ineffectiveness of all three gases in sufficiently depressing the crystallization temperature of the material, thus, presenting processing challenges in foaming. Significant gas loss occurred during the foaming process, resulting in poor blowing agent efficiency; this suggests further rheological modification of the polyester material for improved melt strength and use of annular dies instead of the flat sheet dies.

APPENDIX A

EXPERIMENTAL DATA FROM EXPERIMENTS IN THE SINGLE SCREW EXTRUDER

A-1 Measurement of Gas Solubility in PS (Screw Speed: 15 rpm; Feeder: 20 rpm)

CO_2 at 190°C

Run No.	Window press. (kPa)	Average gas flow rate (cc[STP]/m)	Solubility (cc[STP]/g•kPa)
z101598a	1060.8	77.0	4.56
z101598b	1089.2	74.5	4.41
z101598c	1868.4	132.2	7.82
z101598d	1792.4	11.6	6.72
z101598e	1618.1	119.1	7.05
z102298a	1474.2	76.5	4.53
z102298b	1484.4	78.5	4.65
z102298d	2399.4	164.9	9.76
z102398a	3712.5	202.6	11.99
z102398b	3678.1	195.2	11.55
z102398c	2206.9	192.4	11.39
z102798a	1397.3	74 8	4.43
z102798b	1385.1	65.8	3.90
z102898a	2067.0	124.9	7.39
z102898b	2128.8	133.2	7.88
z102898c	2793.5	157.5	9.32
z102898d	2743.8	161.1	9.53
z102998a	3421.7	217.5	12.87
z102998d	4132.0	255.2	15.10

CO_2 at 215°C

Run No.	Window press. (kPa)	Average gas flow rate (cc[STP]/m)	Solubility (cc[STP]/g•kPa)
z213-1797a	1345.5	20.2	1.98
z213-1797b	2171.3	49.2	4.82
z213-1797c	2777.8	72.6	7.12
z213-1797d	3412.0	92.7	9.09
z213-1797e	4246.0	133.0	13.04
z213-1797f	5420.5	151.4	14.84

N_2 at 190°C

Run No.	Window press. (kPa)	Average gas flow rate (cc[STP]/m)	Solubility (cc[STP]/g•kPa)
z101298a	1297.0	38.0	1.33
z101298b	1295.9	38.3	1.34
z101298c	2615.2	76.7	2.69
z101298d	2732.7	79.6	2.79
z101398a	4179.7	119.6	4.19
z101398d	5946.8	153.2	5.36
z101398e	5819.1	156.7	5.49
z101398c	5490.8	177.8	6.22
z101498a	2240.3	55.8	1.95
z101498b	2232.2	57.6	2.02
z101498c	3681.1	105.3	3.69
z101498d	3649.7	105.9	3.71

N_2 at 215°C

Run No.	Window press. (kPa)	Average gas flow rate (cc[STP]/m)	Solubility (cc[STP]/g•kPa)
Z092901a	1965.7	21.2	1.24
Z092901b	1675.9	23.2	1.36
Z092901c	1581.7	26.4	1.54
Z100198a	2784.4	52.1	3.05
Z100198b	4244.5	85.1	4.98
Z100198c	4285.0	80.1	4.68
Z100198d	4174.6	79.5	4.65
Z100198e	3945.6	83.3	4.87
Z100298a	876.5	7.40	0.43
Z100298b	5985.3	112.8	6.60
Z100298c	5752.2	115.7	6.76

Ar at 215°C

Run No.	Window press. (kPa)	Average gas flow rate (cc[STP]/m)	Solubility (cc[STP]/g•kPa)
z100598a	887.6	16.6	0.99
z100598b	911.9	17.3	1.03
z100598c	1696.2	44.1	2.62
z100598d	1848.2	41.7	2.48
z100598e	3320.4	78.6	4.68
z100898d	3336.6	103.0	6.06
z100898c	3410.6	102.6	6.04
z100898b	5038.9	136.9	8.06
z100998a	2509.8	77.3	4.57
z100998d	5421.9	188.0	11.12

A-2 Measurement of Gas Solubility in PET (Screw Speed: 15 rpm; Feeder: 20 rpm)

CO_2 at 270°C

Run No.	Window press. (kPa)	Average gas flow rate (cc[STP]/m)	Solubility (cc[STP]/g•kPa)
PET-CO2_270a	1137.3	34.1	1.23
PET-CO2_270b	1989.3	92.5	3.34
PET-CO2_270c	2067.9	115.5	4.17
PET-CO2_270d	2757.1	167.0	6.03
PET-CO2_270e	3343.0	213.8	7.72

CO_2 at 290°C

Run No.	Window press. (kPa)	Average gas flow rate (cc[STP]/m)	Solubility (cc[STP]/g•kPa)
PET-CO2_290a	1268.3	27.7	0.97
PET-CO2_290b	1820.4	62.0	2.17
PET-CO2_290c	2447.0	141.0	4.93
PET-CO2_290d	3322.4	195.9	6.85
PET-CO2_290e	3937.9	223.8	7.83

N_2 at 290°C

Run No.	Window press. (kPa)	Average gas flow rate (cc[STP]/m)	Solubility (cc[STP]/g•kPa)
PET-N2_290a	999.1	13.2	0.46
PET-N2_290b	1564.5	22.5	0.78
PET-N2_290c	2288.9	32.5	1.13
PET-N2_290d	3170.5	49.0	1.70
PET-N2_290e	4086.4	67.1	2.33
PET-N2_290f	4654.9	82.1	2.85

Ar at 270°C

Run No.	Window press. (kPa)	Average gas flow rate (cc[STP]/m)	Solubility (cc[STP]/g•kPa)
PET-Ar_270a	1190.4	25.2	0.85
PET-Ar_270b	1690.8	42.9	1.45
PET-Ar_270c	2378.0	65.4	2.21
PET-Ar_270d	3273.4	95.3	3.22
PET-Ar_270e	3933.0	120.8	4.08

Ar at 290°C

Run No.	Window press. (kPa)	Average gas flow rate (cc[STP]/m)	Solubility (cc[STP]/g•kPa)
PET-Ar_290a	1213.8	20.0	0.68
PET-Ar_290b	1924.5	40.6	1.38
PET-Ar_290c	2657.9	69.7	2.37
PET-Ar_290d	3356.8	90.0	3.06
PET-Ar_290e	4106.8	126.7	4.31

APPENDIX B

EXPERIMENTAL DATA FROM EXPERIMENTS IN THE TWIN-SCREW EXTRUDER (CO_2 in PS at 215°C)

B-1 Fixed Screw Speed (30 rpm), Varying Polymer Throughput

Polymer Throughput = 2.40 kg/h

Run No.	Gas Inj. press. (kPa)	Window press. (kPa)	Average gas flow rate (cc[STP]/m)	Solubility (cc[STP]/g•kPa)
z032799a	858.9	1187.0	132.2	3.50
z032799b	839.6	1186.3	118.4	3.13
z032799d	1127.0	1526.1	171.8	4.54
z032999a	593.5	861.6	91.1	2.17
z032999c	1660.5	2100.0	258.2	6.16
z032999d	1655.7	2060.3	259.6	6.20
z032999f	2229.8	2688.9	321.1	7.66

Polymer Throughput = 3.74 kg/h

Run No.	Gas Inj. press. (kPa)	Window press. (kPa)	Average gas flow rate (cc[STP]/m)	Solubility (cc[STP]/g•kPa)
z032399a	1164.9	1523.3	248.2	3.98
z032399b	1160.8	1506.1	258.4	4.15
z032399c	1441.3	1843.2	326.7	5.24
z032399d	1441.3	1857.6	330.8	5.31
z032399e	1721.8	2178.8	377.1	6.05
z032399f	1718.4	2173.3	382.7	6.14
z032499a	762.4	994.6	179.3	2.88
z032499b	758.2	1002.2	181.4	2.91
z032499c	765.1	1032.6	169.2	2.32

Polymer Throughput = 4.97 kg/h

Run No.	Gas Inj. press. (kPa)	Window press. (kPa)	Average gas flow rate (cc[STP]/m)	Solubility (cc[STP]/g•kPa)
z032599a	770.6	1116.6	231.6	2.80
z032599b	770.6	1123.5	232.2	2.80
z032599c	956.0	1343.4	282.2	3.41
z032599d	945.7	1348.9	284.6	3.44
z032599e	1193.2	1590.9	344.1	4.16
z032599f	1187.6	1604.7	347.9	4.20
z032599g	1371.0	1750.8	369.3	4.46
z032599h	1367.5	1757.7	367.6	4.44

Polymer Throughput = 6.12 kg/h

Run No.	Gas Inj. press. (kPa)	Window press. (kPa)	Average gas flow rate (cc[STP]/m)	Solubility (cc[STP]/g•kPa)
z040399a	1064.9	1411.7	333.4	3.24
z040399b	1058.1	1421.3	338.9	3.29
z040399c	1346.2	1664.6	376.6	3.66
z040399d	1343.4	1671.5	387.1	3.76
z040399e	1617.8	1946.5	450.6	4.37
z040399f	1599.8	1975.5	447.3	4.34
z040599a	761.7	1070.5	267.7	2.66
z040599b	751.3	1063.6	263.6	2.62

B-2 Fixed Polymer Throughput (3.76 kg/h), Varying Screw Speed

Screw Speed = 60 rpm

Run No.	Gas Inj. press. (kPa)	Window press. (kPa)	Average gas flow rate (cc[STP]/m)	Solubility (cc[STP]/g•kPa)
z033099e	1130.4	1513.0	260.4	24.17
z033099f	1127.0	1526.8	262.7	24.39
z033199a	1519.9	1936.2	331.0	30.93
z033199b	1511.6	1942.4	322.8	31.03
z033199g	1828.7	2383.6	405.4	38.08
z033199h	1825.2	2338.1	403.8	37.35

Screw Speed = 90 rpm

Run No.	Gas Inj. press. (kPa)	Window press. (kPa)	Average gas flow rate (cc[STP]/m)	Solubility (cc[STP]/g•kPa)
Z033099a	725.8	1114.6	179.6	17.80
Z033099b	721.7	1102.9	177.6	17.62
Z033099g	1120.8	1493.7	248.5	23.86
Z033099h	1101.5	1482.0	251.8	23.67
z033199c	1492.3	1950.7	342.0	31.16
z033199d	1490.2	1959.0	330.1	31.29
z033199e	1839.7	2283.6	411.1	36.48
z033199f	1843.8	2293.3	412.8	36.63
z033099c	701.0	1072.5	170.8	17.13
z033099d	707.2	1060.8	169.8	16.95

Screw Speed = 120 rpm

Run No.	Gas Inj. press. (kPa)	Window press. (kPa)	Average gas flow rate (cc[STP]/m)	Solubility (cc[STP]/g•kPa)
z040199a	737.5	1086.3	169.1	2.75
z040199b	725.1	1093.2	165.9	2.70
z040199c	1051.9	1474.4	231.0	3.76
z040199d	1046.3	1483.3	230.3	3.74
z040199e	1405.5	1870.7	302.1	4.91
z040199f	1397.9	1852.1	302.5	4.92
z040199g	1724.6	2187.1	368.6	5.99
z040199h	1721.8	2219.5	360.0	5.85
z040199i	2025.1	2529.0	410.9	6.68
z040199j	2021.7	2523.5	402.5	6.54

B-3 Special Run: High Screw Speed (120 rpm) and High Polymer Throughput (6.04 kg/h)*

Run No.	Gas Inj. press. (kPa)	Window press. (kPa)	Average gas flow rate (cc[STP]/m)	Solubility (cc[STP]/g•kPa)
z040599c	774.8	1066.3	258.2	2.56
z040599d	780.3	1097.3	258.8	2.57
z040599e	1082.9	1406.1	347.3	3.45
z040599f	1076.0	1425.4	351.1	3.49
z040599g	1455.8	1755.6	425.0	4.22
z040599h	1449.6	1772.2	435.0	4.32

* Melt temperature elevated to 220°C

B-4 Experimental Results on the Effects of Nucleating Agents (Talc) Concentration (Screw Speed: 30 rpm; Polymer throughput: 2.40 kg/h)

Talc Concentration = 0.3wt.%

Run No.	Gas Inj. press. (kPa)	Window press. (kPa)	Average gas flow rate (cc[STP]/m)	Solubility (cc[STP]/g•kPa)
z040999c	1524.8	1550.9	163.0	4.47
z040999d	1530.1	1519.2	165.1	4.52
z040999e	1945.7	2156.1	248.4	6.81
z040999f	1926.5	2103.7	249.8	6.84
z041299a	2086.4	2681.3	277.9	7.61
z041299b	2090.0	2573.8	281.0	7.70
z041299c	2476.9	3474.7	345.7	9.47
z041299d	2477.1	3429.2	341.5	9.36
z041299e	2448.7	3357.5	336.0	9.21

Talc Concentration = 0.1wt.%

Run No.	Gas Inj. press. (kPa)	Window press. (kPa)	Average gas flow rate (cc[STP]/m)	Solubility (cc[STP]/g•kPa)
z040799a	796.1	1138.0	97.1	2.56
z040799b	798.9	1144.2	106.4	2.80
z040799c	1144.9	1501.3	133.9	3.52
z040799d	1138.7	1464.0	137.1	3.61
z040799e	1559.9	1902.4	172.9	4.55
z040799f	1561.9	1895.5	173.5	4.57
z040899a	2030.6	2481.4	302.6	7.86
z040899b	2007.9	2467.6	309.4	8.04
z040899c	2482.8	2975.0	330.3	8.58
z040899d	2475.9	2968.8	341.9	8.88
z040899e	2870.9	3312.7	365.3	9.49
z040899f	2860.5	3293.4	358.8	9.32
z040999a	845.1	1148.4	107.2	2.94
z040999b	848.5	1146.3	108.5	2.97

APPENDIX C

EXPERIMENTAL DATA FROM EXTRUSION FOAMING OF PET IN THE KILLION SINGLE SCREW EXTRUDER

Blowing Agent	N_2	N_2	N_2	N_2	Ar	Ar	Ar	Ar	CO_2	CO_2	CO_2	CO_2
Gas Inj. Press.(kPa)	2090	2760	4210	5540	1380	2760	4160	5510	1430	3050	4040	5340
Melt Press.(kPa)	3240	5030	5375	7225	3240	5030	5375	7225	8550	7470	5735	9200
Melt Temp (^oC)	265.0	262.0	261.5	261.6	262.8	261.0	260.0	260.0	260.2	259.0	259.0	258.4
Gas Flow (scm^3/min)	17.8	13.9	25.6	80.9	30.3	69.8	130.0	157.0	66.7	219.0	301.7	394.0
Density (g/cm^3)	0.87	0.94	0.72	0.80	0.88	0.79	0.81	0.89	1.23	0.68	0.88	0.74
Cell Size (mm)	0.30	0.27	0.25	0.20	0.35	0.32	0.29	0.18	0.15	0.43	0.18	0.20
% Cryst.	8.06	8.24	9.50	12.31	8.29	4.50	7.17	7.94	7.60	6.45	9.25	9.57

REFERENCES

Al-Ghatta, H. and T. Severini, *Proc. 54th SPE ANTEC*, pp1846, 1996.

Al-Ghatta, H.,T. Severini and L. Astarita, *US 5,422,381*, 1995.

Amon, M. and C. D. Denson, "A Study of Dynamics of Foam Growth of Closely Spaced Spherical Bubbles", *Polym. Eng. Sci.*, Vol.24, No.13, pp1026-1034, 1984.

Anonymous, "Acceptable Exposure Limit Lowered", Health Hazard Alert, Office of Health, U.S. Department of Energy, Washington, DC 20585, Issue 92-1, September, 1992.

Anonymous, SNAP Final Rule, 40 CFR Parts 9 and 82, U.S. EPA, March 18, 1994.

Anonymous, "Stratospheric Ozone Protection Q&A", US EPA, last revised on June 23, 1997.

Berens, A. R. and G. S. Huvard, in "*Supercritical Fluid Science and Technology*", Chapter 14, ACS, Washington, DC, 1989.

Biesenberger, J. A. and G. Kessidis, "Devolatilization of Polymer Melts in Single-Screw Extruders", *Polym. Eng. Sci.*, Vol.22, No.13, pp832-835, 1982.

Biesenberger, J. A. and D. H. Sebastian, *Principles of Polymerization Engineering*, Wiley, New York 1983.

Biesenberger, J. A., ed., *Devolatilization of Polymers*, Hanser, Munich, 1983.

Biesenberger, J. A and S. T. Lee, *Polym. Eng. Sci.*, Vol. 26, pp982, 1986.

Biesenberger, J. A and S. T. Lee, *Polym. Eng. Sci.*, Vol. 27, pp510, 1987.

Biesenberger, J. A, S. K. Dey and J. Brizzolara, "Devolatilization of Polymer Melts: Machine Geometry Effects", *Proceedings of the 1990 SPE ANTEC*, pp129-131, 1990.

Boone, G, *Proc. Foam Conference 96*, LCM Public Relations, pp145-157, Somerset, NJ, December 10-12, 1996.

Brockmerer, N. F., R. W. McCoy, and J. A. Meyer, "Gas Chromatographic Determination of Thermodynamic Properties of Polymer Solutions. I. Amorphous Polymer Systems", *Macromolecules*, Vol.5, pp464, 1972.

Brown, S. B., in M. Xanthos, Ed., *"Reactive Extrusion: Principles and Practice"*, Carl Hanser Verlag, Munich, New York, pp161-176, 1992.

Caron, et al., "Rheology, Solubility and Monitoring Systems for Foam Extrusion", Presented at the FoamTech'97 Conference, Toronto, Canada, August, 1997.

Cheung, L. K., C. B. Park and A. H. Behravesh, *Proceedings of the 55th SPE ANTEC*, pp1941, 1996.

Collins, G. P., C. D. Denson and G. Astarita, "Determination of Mass Transfer Coefficients for Bubble-Free Devolatilization of Polymeric Solutions in Twin-Screw Extruders", *AIChE J.*, Vol.31, pp1288-1296, 1985.

Colton, J. S. and N. P. Suh, "The Nucleation of Microcellular Thermoplastic Foams with Additives, Part II: Experimental Results and Discussion", *Polym. Eng. Sci.*, Vol.27, No.7, pp493-499, 1987.

Coughlin, R. W and G. P. Caneveri, *AIChE J.*, Vol. 15, pp560, 1969.

Dagli, S. S., R. F. Staats-Westover and J. A. Biesenberger, "Measurement of Gas Solubility and Relationship to Extruded Foam Properties: A New Apparatus and Some Data on Nitrogen in Polyolefins", *Proceedings of the 1989 SPE ANTEC*, pp889-890, 1989.

Daigneault, L. E., Y. P. Handa, B. Wong and L.M. Caron, "Solubility of Blowing Agents HCFC 142 B, HFC134A, HFC 125 and Isopropanol in Polystyrene", *Proceedings of the 1997 SPE ANTEC*, pp1983-1987, 1997.

Dey, S. K., "Measurement of Solubility of Gases in Polymer Melts", *Adv. Polym Technol.*, Vol. 10, pp317, 1990.

Dey, S. K., C. Jacob and J. A. Biesenberger, "Effect of Physical Blowing Agents on Crystallization Temperature of Polymer Melts", *Proceedings of 1994 SPE ANTEC*, San Francisco, CA, pp2197-2198, 1994.

Dey, S. K., C. Jacob and M. Xanthos, *J. Vinyl and Addit. Technol.*, Vol. 2, pp48, 1996a.

Dey, S. K., P. Natarajan, M. Xanthos and M. D. Braathen, *J. Vinyl and Addit. Technol.*, Vol. 2, pp339, 1996b.

Dey, S. K., private communications, Polymer Processing Institute, Hoboken, NJ, June 1997.

Duda, J. L. and J. S. Vrentas, "Diffusion in Atactic Polystyrene Above the Glass Transition", *J. Polym. Sci.*, Vol.6, pp675, 1968.

Duda, J. L., G. K. Kimmerly, W. L. Sigelko, and J. W. Vrentas, "Sorption Apparatus for Diffusion Studies with Molten Polymers", *Ind. Eng. Chem. Fundamentals*, Vol.12, pp133-, 1973.

Durrill, P. L and R. G. Griskey, "Diffusion and Solution of Gases in Thermally Softened or Molten Polymers-Part I. Development of Technique and Determination of Data", *A.I.Ch.E. J.*, Vol.12, No.6, pp1147-1151, 1966.

Durrill, P. L and R. G. Griskey, "Diffusion and Solution of Gases in Thermally Softened or Molten Polymers-Part II. Relation of Diffusivities and Solubilities with Temperature, Pressure and Structural Characteristics", *AIChE. J.*, Vol.15, pp106-110, 1969.

Elkovitch, M. D., L-J Lee and D. L. Tomasko, *Proceedings of 56th SPE ANTEC*, Atlanta, GA, pp1855, 1998.

Elkovitch, M. D., L-J Lee and D. L. Tomasko, *Proceedings of 57th SPE ANTEC*, New York, NY, pp2811, 1999.

Faridi, N., Unpublished experimental results, Polymer Processing Institute, Hoboken, NJ, May 1998.

Flory, P. J., *Principles of Polymer Chemistry*, p.495, Cornell University Press, Ithaca, N.Y. 1953.

Foster, R. W. and J. T. Lindt, "Bubble Growth Controlled Devolatilization in Twin-Screw Extruders", *Polym. Eng. Sci.*, Vol. 29, pp178-185, 1989.

Gabriele, M. C., "New Foam Extrusion Technology is 'Environmentally Friendly'", *Plastics World*, Vol.42, No.5, pp30-31, 1996.

Grace, H. P., *Chem. Eng. Commun.*, Vol. 14, pp225, 1982.

Han, C. D., "*Multiphase Flow in Polymer Processing*", Chapter 6, pp257-338, Academic Press, New York, 1981.

Han, J. H. and C. D. Han, *J. Polym. Sci.*, Vol.28, pp711, 1990.

Handa, Y. P, P. Kruus and M. O'Neill, *J. Polym. Sci., Part B: Polym. Phys.*, Vol.34, pp2635, 1996.

Hansen, R. H. and W. M. Martin, *Ind. Eng. Chem., Res. Dev.*, Vol. 3, pp137, 1964.

Hansen, R. H. and W. M. Martin, *J. Polym. Sci., Part B*, Vol. 3, pp325, 1965.

Jacob, C. and S. K. Dey, "Inert Gases as Alternatives Blowing Agents for Extruded Low Density Polystyene Foam", *J. Cell. Plast.*, Vol.31, pp38-47, 1995.

Kamiya, Y, T. Hirose, K. Mizoguchi and Y. Natio, *J. Polym. Phys*, Vol.24, pp1525-, 1986.

Kesari, S., S. Kaplia and G. Bertrand, "Assessment of Freon Release from Polyurethane Foams", *Proceedings of the 10th Annual Conference on Hazardous Waste Research*, Manhattan, KS, pp79, 1995.

Khemani, K. C., "Extruded Polyester Foams", in K. C. Khemani Ed., "Polymeric Foams", Chapter 5, American Chemical Society, Washington D. C., pp 54-80, 1997.

Klempner, D. and K. C. Frisch, Eds., *Handbook of Polymeric Foams and Foam Technology* , Hanser Publisher, 1991.

Kumar, V. and J. E. Weller, "Bubble Nucleation in Microcellular Polycarbonate Foams", *Polymer Material Science and Engineering*, Vol.67, pp501-502, 1992.

Latinen, G., *ACS Adv. Chem. Series*, Vol.34, pp235, 1962.

Lee, M, C. Tzoganakis and C. B. Park, *Proc. 56th SPE ANTEC*, Atlanta, GA, pp2570, 1998.

Lee, M, C. Tzoganakis and C. B. Park, *Proc. 57th SPE ANTEC*, New York, NY, pp2806, 1999.

Lee, S. T., "Shear Effects on Thermoplastic Foam Extrusion", *Polym. Eng. Sci.*, Vol.33, pp418-422, 1993.

Lee, S. T., "More Experiments on Thermoplastic Foam Nucleation", *J. Cell. Plast.*, Vol.30, pp444-453, 1994.

Levitskiy, S. P. and Z. P. Shulman, *Bubbles in Polymeric Liquids: Dynamics and Heat-Mass Transfer*, Technomic Publishing, PA, 1995.

Lundberg, J. L., M. B. Wilk and M. J. Huyett, *I&EC Fundamentals*. Vol.2, No.1, pp37-43, 1963.

Maloney, D. P. and J. M. Prausnitz, "Solubilities of Ethylene and Other Organic Solutes in Liquid, Low - Density Polyethylene in the Region 124°C to 300 °C", *AIChE J.*, Vol.22, pp74, 1976.

Micheals, A. S., W. R. Vieth and J. A. Barrie, "Solution of Gases in Polyethylene Terephthalate", *J. Appl. Physics*, Vol.34, No.1, pp1-12, 1963a.

Micheals, A. S., W. R. Vieth and J. A. Barrie, *J. Appl. Physics*, Vol.34, No.1, pp20, 1963b.

Moulinie, P., R. Gendron and L. E. Daigneault, "Gas Solubility as a Guide to Physical Blowing Agent Selection", *Proceedings of the Foamplas'98 Conference*, pp123-142, 1998.

Newitt, D. M. and E. W. Weale, *J. Chem. Soc.* (London), pp1541, 1948.

Park, C. B and L. K. Cheung, *Polym. Eng. Sci.*, Vol. 37, pp1, 1997.

Ramesh, N. S., D. H. Rasmussen and G. A. Cambell, "Numerical and Experimental Studies of Bubble Growth During Microcellular Foaming Process", *Polym. Eng. Sci.*, Vol.31, pp1657-1664, 1991.

Ramesh, N. S. and N. Malwitz, "Bubble Growth Dynamics in Olefinic Foams", in *Polymeric Foams*, Ed. By Khemani, K. C., ACS, Chapter 14, pp206-213, 1997.

Rein, D. H., Csernica, J., Baddour, R. F., and Cohen, R. E., "CO_2 Diffusion and Solubility in a Polystyrene-Polybutadiene Block Copolymer with a Highly Oriented Lamellar Morphology", *Macromolecules*, Vol. 23, pp4456 , 1990.

Roberts, G. W., "A Surface Renewal Model for the Drying of Polymers During Screw Extrusion", *AIChE J.*, Vol.16, No.5, pp878-882, 1970.

Sato, Y., M. Yurugi, K. Fujiwara, S. Takishima and H. Masuoka, "Solubilities of Carbon Dioxide and Nitrogen in Polystyrene under High Temperature and Pressure", *Fluid Phase Equilibria*, Vol.125, pp129-138, 1996.

Stiel, I. L. and D. F. Harnish, "Solubility of Gases and Liquids in Molten Polystyrene", *AIChE J.*, Vol.22, pp117, 1976.

Street, J. R., *Trans. Soc. Rheol.*, Vol.12, pp103, 1968.

Street, J. R. A. L. Fricke and L. P. Reiss, *Ind. Eng. Chem. Fund.* Vol.10, pp54-64, 1971.

Tadmor, Z. and C. G. Gogos, *Principles of Polymer Processing*, John Wiley & Sons, New York, 1979.

Throne, J. L., "Is Your Thermoplastic Polymer Foamable?", *Proceedings of Foam Conference '96*, Somerset, NJ, pp2-14, 1996.

Todd, D. B., private communications, Polymer Processing Institute, Newark, NJ, November 1999.

Toor, H. L. and Marchello, J. M., "Film-Penetration Model for Mass and Heat Transfer", *AIChE Journal*, Vol.4, pp97-101, 1958.

Tukachinsky, A., Y. Talmon and Z. Tadmor, "Foam-Enhanced Devolatilization of Polystyrene Melt in a Vented Extruder", *AIChE J.*, Vol. 40, pp675, 1994.

Van Krevelen, D. W., *Properties of Polymers*, Chapter 18, 2nd Ed., Elsevier, Amsterdam, 1976.

Wang, W. C, E. J. Kramer and W. H. Sachse, *J. Polym. Sci., Polym. Phys. Ed.*, Vol.20, pp1371, 1982.

Wissinger, R. G. and M.E. Paulaitis, *J. Polym. Sci.: Part B: Polym. Phys*, Vol.29, pp631, 1991.

Wong, B and Y. P. Handa, "A High-Pressure Electroblance Based In-Situ Technique for Determining the Solubility and Diffusivity of Gases in Polymers", *Proceedings of 1997 SPE ANTEC*, Toronto, Canada, pp1979-1982, 1997.

Xanthos, M., Q. Zhang, S. K. Dey, Y. Li, U. Yilmazer and M. O'Shea, "Effects of Resin Rheology on the Extrusion Foaming Characteristics of PET", *Journal of Cellular Plastics*, Vol. 34, pp498-510, 1998.

Xanthos, M., U. Yilmazer, S. K. Dey and J. Quintans, "Melt Viscoelasticity of Polyethylene Terephthalate Resins For Low Density Extrusion Foaming", *Polym. Eng. Sci.*, (in press).

Xie, H. and R. Simha, *Polym. Int.*, Vol. 44, pp348, 1997.

Zhang, Q., unpublished experimental results, New Jersey Institute of Technology, Newark, New Jersey, August 1997.

Zhang, Z. and P.Y. Handa, "CO_2-Assisted Melting of Semicrystalline Polymers", *Macromolecules*, Vol.30, pp8505-8507, 1997.